**CHIMERIC ANTI-CD19 MONOCLONAL ANTIBODIES FOR THE TREATMENT OF PRECURSOR B CELL ACUTE LYMPHOBLASTIC LEUKEMIA**

APPROVED BY SUPERVISORY COMMITTEE

Ellen S. Vitetta, Ph.D.

Rolf Brekken, Ph.D.

William Garrard, Ph.D.

E. Sally Ward, Ph.D.

Nancy E. Street, Ph.D.

***I dedicate this work to my loving husband***

***Allen Tsai,***

***Without whom so much in my life, including this work,***

***would not be possible.***

# CHIMERIC ANTI-CD19 MONOCLONAL ANTIBODIES FOR THE TREATMENT OF PRECURSOR B CELL ACUTE LYMPHOBLASTIC LEUKEMIA

By

LYDIA KAR-YUK TSAI

DISSERTATION

Presented to the Faculty of the Graduate School of Biomedical Sciences

The University of Texas Southwestern Medical Center at Dallas

In Partial Fulfillment of the Requirements

For the Degree of

DOCTOR OF PHILOSOPHY

The University of Texas Southwestern Medical Center at Dallas

Dallas, Texas

June 3, 2009

## ACKNOWLEDGEMENTS

I thank my mentor, Dr. Ellen Vitetta, for her unfaltering guidance and dedication. I am truly honored to have learned science from such a well accomplished and highly respected scientist and about life from a woman who is a leader among men. She has never failed to believe in my potential to become a scientist and has always challenged me to become a better one. My accomplishments in my research and career are to her credit; my failures are my own.

I thank Drs. Xiaoyun Liu and Laurentiu Pop, both of whom have been instrumental to this project. These two exceptional scientists are the brains of this operation, and have helped me tremendously throughout my graduate years. I am deeply grateful to have learned from two amazing teachers in the laboratory, and I thank them especially for their selflessness, infinite kindness, and friendship.

I thank my dissertation committee members Drs. Rolf Brekken, William Garrard, Nancy Street, and Sally Ward for their valuable input to my work. I appreciate their helping me become a better scientist, and have had a pleasure learning from them and working with them.

I thank Drs. Maria-Ana and Victor Ghetie and Dr. Joan Smallshaw. Dr. Smallshaw had helped me get started with the initial molecular biology

work to chimerize HD37, and has continued her support throughout the project. Dr. M.A. Ghetie has taught me HD37 *in vitro* techniques, and Dr. V. Ghetie has taught me about antibodies and immunotoxins. I also learned much through their own work in the laboratory for they are as talented as scientists as they are teachers.

I thank Linda Berry who has a heart of gold and has been one of my greatest cheerleaders and supporters. I am blessed to have come under her guidance and received her endless help throughout the years. I also thank Kristi Gage, Rhonda McCracken, Catherine Holloway, and Erica Garza of the administrative staff in the Cancer Immunobiology Center for their helpfulness and kindness. I thank Karen Kazemzadeh and Priyarama Sen for their support in navigating my way as a graduate student at this University.

I thank my fellow students in the laboratory, Andrew BitMansour for his incredible patience, thoughtfulness, and inspiration; Allison Case for being a confidante and for her continuous encouragement; Pavitra Chakravarty for her infectious spirit and boundless kindness; Praveena Selvaduray, Dr. Kimberly Brooks, and Dr. Elaine Coleman for their wonderful support during these formative graduate years. I have found lasting friendships with these fellow students, which I will cherish for life.

I thank Kelly Mapes, Ayesha Ahmed, Lien Le, Ming-mei Liu, Ryan Willingham, Iliodora Pop, Drew Ivey, John Gu, Steve Ruback, and Nancy Lane for their all of their help in the laboratory. They have made my work possible in so many ways, and I am grateful for their help and friendship.

I thank my friends and family who have supported and encouraged me, listened to my joys and woes, and wished the best for me during my graduate training. I thank the Bhoj's for their invaluable friendship and support. I thank my families in California, the Wu's, Chu's and Tsai's, who have never had any doubt in my abilities and will always support my endeavors.

Last, but certainly not least, I thank my wonderful husband, Allen Tsai. I thank him for his limitless patience, steadfast dependability, and unconditional love. He is an inspiration to me through his many achievements, and his loving support and encouragement have made it possible for me to achieve my goals.

**CHIMERIC ANTI-CD19 MONOCLONAL ANTIBODIES FOR THE TREATMENT OF PRECURSOR B CELL ACUTE LYMPHOBLASTIC LEUKEMIA**

LYDIA KAR-YUK TSAI, Ph.D.

The University of Texas Southwestern Medical Center at Dallas, 2009

Supervising professor: ELLEN S. VITETTA, Ph.D.

Thousands of people are diagnosed with B cell malignancies every year, yet the only FDA-approved immunotherapies for them are based on anti-CD20 monoclonal antibodies (MAbs). However, CD20 is not expressed on precursor B cell acute lymphoblastic leukemia (pre-B ALL),

and CD20 expression is often lost following anti-CD20 immunotherapy. CD19 is a pan B cell membrane antigen that is restricted to the B cell lineage and expressed on B cell lymphomas and pre-B ALLs. Previous studies have shown that a murine anti-human CD19 MAb, HD37, has efficacy in SCID mice with human B cell tumors. Furthermore, homodimers consisting of two conjugated IgG molecules of HD37 are more effective than monomers at inducing tumor cell death. Yet, their large size prevents effective tumor penetration, and normal Fc effector funtions are often not retained. Murine antibodies are also highly immunogenic. Therefore, the objective of this study was to construct, express, and test the *in vitro* and *in vivo* activities of chimeric divalent and tetravalent HD37 MAbs. Both chimeric HD37 MAbs and the murine HD37 MAb were equally effective at mediating antibody dependent cellular cytotoxicity (ADCC) with mouse effector cells. The anti-tumor activities of all three MAbs were identical in SCID mice xenografted with human B cell tumors. However, the chimeric tetravalent MAb has a higher binding affinity and a longer half-life of dissociation than either of the divalent MAbs. Moreover, the chimeric tetravalent MAb mediated ADCC and complement dependent cytotoxicty (CDC) more efficiently than the divalent MAbs when human effector cells and human complement were used. None of the MAbs were cytotoxic to target cells in the absence of

effector cells or complement. These data suggest that 1) the HD37 MAbs effectively extend the mean survival time of SCID mice engrafted with human B cell tumors; 2) more than two of the tetravalent HD37 MAb's binding sites are active; and 3) because *in vitro* results show that the chimeric tetravalent MAb is more effective than the divalent MAbs at mediating ADCC and CDC with human effector cells and complement, the chimeric tetravalent HD37 MAb could be superior to the divalent MAbs in humans.

## TABLE OF CONTENTS

## PRIOR PUBLICATIONS

Tsai LK, Liu XY, Pop LM, Vitetta ES. Construction, expression, and evaluation of the anti-tumor activity of chimeric, tetravalent and divalent anti-CD19 monoclonal antibodies. Manuscript in preparation 2009

Tsai LK, Pop LM, Liu XY, Ghetie V, Vitetta ES. An anti-CD19 immunotoxin. Manuscript in preparation 2009

Vaclavkova P, Cao Y, Wu LK, Michalek J, Vitetta ES. A comparison of an anti-CD25 immunotoxin, Ontak and anti-CD25 microbeads for their ability to deplete alloreactive T cells in vitro. Bone Marrow Transplant. 2006 Mar;37(6):559-67

Lee Y, Gough RA, Leung KN, Perkins LT, Pickard DS, Vujic J, Wu LK, Olivo M, Einenkel H. Quartz antenna for radio frequency ion source operation. Review of Scientific Instruments, 1998 Feb;69(2):1023-1025.

## LIST OF FIGURES

## LIST OF TABLES

## LIST OF ABBREVIATIONS

| | |
|---|---|
| **ADCC** | Antibody dependent cellular cytotoxicity |
| **AML** | Acute myeloid leukemia |
| **BC** | B cell |
| **BCR** | B cell receptor |
| **BME** | Beta-mercaptoethanol |
| **BSA** | Bovine serum albumin |
| **CDC** | Complement dependent cytotoxicty |
| **CDR** | Complementarity-determining regions |
| **CH** | Heavy chain constant region |
| **cHD37** | Divalent chimeric HD37 |
| **cHD37-DcVV** | Tetravalent chimeric HD37 |
| **CL** | Light chain constant region |
| **CLL** | Chronic lymphocytic leukemia |
| **CNS** | Central nervous system |
| **dgRTA** | Deglycosylated ricin toxin A chain |
| **DMEM** | Dulbecco's Modified Eagle's Medium |
| **E:T** | Effector to target cell ratio |
| **EGFR** | Epidermal growth factor receptor |

| | |
|---|---|
| **ELISA** | Enzyme linked immunosorbent assay |
| **FBS** | Fetal bovine serum |
| **FcR** | Fc receptor |
| **FDA** | United States Food and Drug Administration |
| **FITC** | Fluorescein isothiocyanate |
| **GVHD** | Graft-versus-host disease |
| **HAMA** | Human anti-mouse antibody |
| **HSCT** | Hematopoietic stem cell transplantation |
| **Ig** | Immunoglobulin |
| **IMDM** | Iscove's Modified Dulbecco's Media |
| **IT** | Immunotoxin |
| **ITAM** | Immunoreceptor tyrosine-based activation motif |
| **ITIM** | Immunoreceptor tyrosine-based inhibition motif |
| **IV** | Intravenously |
| **LAK** | Lymphokine-activated killer |
| **LPS** | Lipopolysaccharide |
| **MAb** | Monoclonal antibodies |
| **MM** | Multiple myeloma |
| **MPT** | Mean paralysis time |
| **MTS** | 3-(4,5-dimethylthiazol-2-yl)-5-(3-carboxymethoxyphenyl)-2-(4-sulfophenyl)-2H-tetrazolium) |

| | |
|---|---|
| **NFκB** | Nuclear factor kappa-B |
| **NHL** | Non-Hodgkin's lymphoma |
| **NK** | Natural killer |
| **p-NPP** | p-Nitrophenyl phosphate disodium salt hexahydrate |
| **PBMC** | Peripheral blood mononuclear cells |
| **PBS** | Phosphate buffered saline |
| **PCR** | Polymerase chain reaction |
| **PI** | Propidium iodide |
| **PI-3** | Phosphatidyl-inositol-3 |
| **PK** | Pharmacokinetics |
| **Pre-B ALL** | Precursor B cell acute lymphoblastic leukemia |
| **RPMI-1640** | Roswell Park Memorial Institute-1640 |
| **SCID** | Severe combined immunodeficient |
| **SDS-PAGE** | Sodium dodecyl sulfate polyacrylamide gel electrophoresis |
| **SPR** | Surface plasmon resonance |
| $T_{1/2}$ | Half life |
| **TCR** | T cell receptor |
| **VEGF** | Vascular endothelial growth factor |
| **VH** | Heavy chain variable region |
| **VL** | Light chain variable region |

**WHO** World Health Organization

# CHAPTER ONE

# Introduction

## A. Hematological Cancers

Hematological cancers are diseases in which abnormal cells of the blood, bone marrow or lymphatic tissues grow aberrantly and spread to many sites in the body. These cancers include various forms of lymphomas, leukemias, and myelomas. Hematological cancers are a major health concern. In 2005, the prevalence of hematological cancers was greater than 800,000, with an incidence of more than 135,000 cases diagnosed in both children and adults, and a death rate of more than 53,000 people in the United States[1]. The risk factors and causes of most hematological cancers are unknown. Despite significant advances in the development of more sensitive detection methods and more effective treatment options, hematological cancers remain a serious health problem both in the United States and worldwide.

Hematological cancers are heterogeneous diseases and can originate from various types of cells in the blood or bone marrow. Cancers of B cell origin comprise a large portion of these malignancies and are very common hematological disorders. This study will focus primarily on B

cell malignancies, particularly precursor B cell acute lymphobloastic leukemia (pre-B ALL) and B cell non-Hodgkin's lymphoma (NHL).

*Acute Lymphoblastic Leukemias*

ALL is a malignant disorder of lymphoid progenitor cells and can be of T cell, mature B cell, or B cell precursor origin, but a vast majority (80-85%) are B cell precursor type[2, 3]. ALL affects thousands of people in the United States every year, and there has been a gradual increase in the incidence of ALL in the past 25 years[4]. There were an estimated 5,430 new diagnoses and 1,460 deaths among adults in 2008[3]. Sixty to 80% are expected to attain complete remission following induction therapy, which consists of combination chemotherapy. Approximately 35% to 40% of adults with ALL can be expected to survive 2 years with aggressive chemotherapy.

ALL is the most common cancer diagnosed in children and represents 23% of all cancer diagnoses among children younger than 15 years of age[5]. There are approximately 2,400 children and adolescents younger than 20 years of age who are diagnosed with ALL each year in the United States. More than 95% of children diagnosed with ALL achieve

remission, and 75% to 85% are leukemia-free for at least 5 years after diagnosis when current treatments are used[6].

There are few identified factors associated with an increased risk of ALL. The primary accepted non-genetic risk factors for ALL are prenatal exposure to x-rays and postnatal exposure to high doses of radiation[5]. Children with Downs syndrome have an increased risk of developing both ALL and acute myeloid leukemia (AML)[7, 8]. Many cases of ALL that develop in children have a prenatal origin. Evidence in support of this comes from observations that antigens from immunoglobulin (Ig) or T-cell receptor (TCR) rearrangements that are unique to each patient's leukemia cells can be detected in blood samples obtained at birth[9, 10].

Based on immunophenotyping, 80-85% of all ALLs are of the early B-cell lineage and are referred to as pre-B ALLs[3]. They are defined by the expression of CD10 (CALLA), CD19, HLA-DR, and cytoplasmic expression of CD79a[6]. Pre-B ALLs are further categorized into four subtypes based on CD10 and cytoplasmic Ig expression: pro-B ALL, which has no surface CD10 or cytoplasmic Ig expression; common pre-B ALL, which expresses CD10 but no surface or cytoplasmic Ig; pre-B ALL, which expresses both CD10 and cytoplasmic (but not surface) Ig; and transitional pre-B ALL, which expresses membrane Ig μ chain without light chain[2]. Approximately three-quarters of patients with precursor B-cell ALL

have the common precursor B-cell immunophenotype and have the best prognosis.

ALL treatments typically consists of three phases, a remission-induction phase, an intensification (or consolidation) phase, and continuation therapy to eliminate residual disease[11]. The average length of treatment varies between 1.5 to 3 years. All three phases of treatment involve combination systemic chemotherapy. Several common classes of chemotherapeutic drugs approved by the U.S. Food and Drug Administration (FDA) for the therapy of various cancers include DNA alkylating agents, platinum compounds, anti-metabolites, topoisomerase interactive agents, and anti-microtubule agents. Treatment of ALL is also directed to the central nervous system (CNS) to prevent relapse attributable to leukemic cells sequestered at this site[11]. Chemotherapy and/or radiation therapy are common forms of treatment in the CNS. Because chemotherapeutic agents typically affect all rapidly proliferating cells by interfering with DNA replication or cell division, both cancerous and rapidly dividing, healthy cells are affected. Therefore, treatment with chemotherapy is typically associated with a variety of minor and severe side effects, including myelosuppression, uric acid build up in the blood, and anemia. Myelosuppression is the greatest concern because it can

lead to immunosuppression and subsequent infections, anemia, and deficient wound healing[12].

Allogeneic hematopoietic stem cell transplantation (HSCT) is the most aggressive form of treatment for ALL. Patients with high-risk forms of ALL, such as individuals with Philadelphia chromosome-positive disease, and those with a poor response to initial treatment may benefit from allogeneic HSCT. However, this treatment is considered to be high-risk with significant morbidity and mortality. Other risks include graft-versus-host disease (GVHD) and immunosuppression.

Despite the high rate of remission, the current treatment modalities are not curative in all ALL cases. Furthermore, chemotherapy and HSCT are associated with a systemic toxicity and general immunosuppression. Therefore, better strategies are needed for the treatment of ALL.

*B Cell Non-Hodgkin's Lymphomas*

Lymphoma is a heterogeneous group of cancers that develop from the uncontrolled proliferation of B cell or T cells, which are normally a part of the adaptive immune system. There are two main types of lymphoma—Hodgkin's lymphoma, which develops from Reed-Sternberg B cells, and NHLs, which includes all other lymphomas. In 1995, the World Health

Organization (WHO) proposed using the Revised European American Lymphoma Classification (REAL) system to better classify the different types of lymphomas based on immunologic and genetic techniques, and this classification system is still in effect today[13]. The three major types of lymphomas are Hodgkin's lymphoma (nodular and classical), B cell neoplasms (precursor B cell and peripheral B cell), and T cell and putative natural killer (NK) cell neoplasms (precursor T cell and peripheral T and NK cell). Lymphomas are further categorized as indolent (low-grade) or aggressive (high-grade). Although NHLs can be of B, T or NK cell origins, over 90% of lymphomas are of B cell origin. B cell NHLs include Burkitt's lymphoma, diffuse large B cell lymphoma, follicular lymphoma, immunoblastic large cell lymphoma, precursor B-lymphoblastic lymphoma, and mantle cell lymphoma. Approximately 4% of all cancers diagnosed are NHLs, and there were an estimated 66,000 new cases in the U.S. in 2008[5]. The incidence of NHL has nearly doubled in the last 55 years, and it continues to climb. It is estimated that over 500,000 people live with or have a history of NHL, and 19,000 people died in 2008 from NHL. While some subtypes of NHL are relatively common in children, over 95% of NHLs occur in adults. The risk of developing NHL also increases in individuals who are immunosuppressed due to organ transplant, have an autoimmune disease, or have been infected with certain viruses such as

human immunodeficiency virus, hepatitis C virus, or Epstein-Barr virus. However, the specific risk associations and epidemiology vary according to the subtype of NHL[14].

Despite the continued increase in incidence, the mortality rate of patients with NHL is steadily decreasing. Although the mortality rate varies greatly depending upon the originating cell type and the stage of disease, the average five and ten-year survival rates are currently 63% and 49%, respectively[14]. The observed decrease in the mortality rate over the last decade is thought to be due to improvements in the therapeutic options for patients with NHL.

Treatment of NHL depends on the histologic stage and type. There are four stages of NHL (Stage I-IV) based on how widespread the cancer is. Chemotherapy is often administered to patients and given in cycles several weeks apart for 6-10 months. It is usually used in combination with several drugs. A commonly administered combination is R-CHOP, which includes Rituxan™, cyclophosphamide, doxorubicin, vincristine, and prednisone, for some types of NHL. Because high doses of chemotherapy are used, normal blood cells counts drop dramatically thereby increasing the risk of myelosuppression and general immunosuppression. Therefore, growth factors to increase red blood cell and neutrophil numbers such as

Aranesp™, Procrit™, Neupogen™, or Leukine™ are often administered to patients between rounds of chemotherapy.

Rituxan™ is a monoclonal antibody (MAb) therapy that specifically targets $CD20^+$ B cells. Other biological therapies effective in the treatment of some NHL types include the anti-CD52 MAb Campath™, the radiolabeled anti-CD20 antibodies Bexxar™ and Zevalin™, and IFN-α cytokine therapy. MAb therapy can be given in combination with other forms of treatment or administered alone.

Radiation therapy is sometimes administered along with chemotherapy when there are very large masses of lymphoma cells in a small area of the body or when large lymph nodes are pressing on an organ and chemotherapeutic drugs are not sufficient for controlling tumor cell growth. Because lymphoma is usually a disseminated cancer, radiotherapy isn't the only treatment option for NHL.

Allogeneic HSCT is another form of treatment for NHL. However, due to the high risk associated with allogeneic HSCTs, the patient’s type of NHL, age and overall health are evaluated. Nonmyeloablative allogeneic HSCT, which does not use high-dose chemotherapy to eliminate the host hematopoietic system and minimizes GVHD, is emerging as a new form of treatment especially for older patients who are not able to undergo regular HSCT. Another emerging form of therapy is

the combination of high-dose chemotherapy with autologous stem cell infusions. However, this type of treatment does not give patients longer disease-free periods than standard-dose chemotherapy without stem cell transplant and is therefore not viewed as curative.

As in the case of ALL, the current treatment options are not curative for all types of NHLs, and there are many side effects that are associated with chemotherapy or radiotherapy. Better treatment options with less systemic toxicity and adverse side effects are needed.

## B. Monoclonal Antibodies for the Treatment of Cancer

The production of monoclonal antibodies was described by Kohler and Milstein in 1975[15]. Their technique involved the immortalization of MAb-secreting cells from mice immunized against desired antigens and the subsequent screening of the hybridoma cells for reactivity with the target antigen. In the last 34 years, numerous advances in genetic and protein engineering have enhanced the therapeutic potential of MAbs, either naked or conjugated to drugs, in their use against cancers or viral and inflammatory diseases. Currently, there are nine MAbs and immunoconjugates approved by the FDA for the treatment of cancer, and hundreds more are currently being evaluated in clinical trials[16, 17].

### *Specificity*

An important advantage of MAb therapy over other cancer treatments such as chemotherapy or radiotherapy is the specificity of the MAb. Paul Ehrlich described antibodies as ‘magic bullets’ that would specifically trace and kill microbes and tumor cells[18]. Indeed, MAbs are highly specific for their antigen. A variety of protein or carbohydrate receptors on the surface of cancer cells are potential targets for antibody-

directed therapies, although the most clinically useful are ones that are uniquely expressed by cancer cells, expressed at higher levels than normal cells, or antigens limited to one cell type or lineage. Therefore, MAbs can be used to specifically target and kill cancer cells through a variety of mechanisms. Although MAbs may also react with some normal cells, their selective activity provides therapeutic efficacy with fewer side effects than conventional chemotherapy or radiation therapy thus decreasing systemic toxicity.

*Mechanisms of Action*

Antibodies can exert anti-tumor effects through multiple mechanisms that are not mutually exclusive. Antibodies can work by inducing apoptosis or cell growth arrest[19], interfering with ligand-receptor interactions[20], or preventing the expression of proteins that are critical to the neoplastic phenotype[17]. Promising results have been obtained using an antibody against CTLA-4, an inhibitory receptor that modulates cellular immunity and thereby regulates T cell responses[21, 22]. MAbs have also been developed to target the growth of the cancers instead of the cancer itself. For example, Avastin™ is thought to starve tumor cells by preventing the binding of vascular endothelial growth factor (VEGF) to its

receptor and thus inhibiting the formation of new vasculature[23]. Other antibodies target receptors whose ligands are growth factors. Erbitux™ binds to epidermal growth factor receptor (EGFR) and slows tumor growth by blocking epidermal growth factor from binding to its receptor, resulting in the inhibition of tumor cell growth and proliferation, angiogenesis, and metastasis[24]. These blocking or regulatory antibodies slow down tumor growth and might enhance clinical responses when combined with chemotherapy or other tumor-specific antibodies. However, this modulation of regulatory and survival signaling pathways alone will not be sufficient to eliminate tumor cells, and the recruitment of secondary immune effector mechanisms is of great importance for the efficiency of antibody therapy[25].

Fc-mediated effector functions of antibodies are the most important effector mechanisms employed by MAbs in cancer therapy, and among these, antibody dependent cellular cytotoxicity (ADCC) is the most common[26]. During ADCC, antibodies bound to specific antigens on tumor cells recruit phagocytic effector cells that express Fc receptors (FcR) specific for the constant region of the antibody, trigger the release of inflammatory mediators, and lyse the tumor cells. Another Fc-mediated effector mechanism is complement dependent cytotoxicity (CDC), which occurs when the first component of the complement cascade, the C1q

protein, binds to cell-bound antibodies and activates the classical complement cascade. This results in the lysis of the tumor cells bound to the antibodies. C1q is capable of binding to the Fc portion of IgM and IgG molecules clustered on the cell surface. The species of origin of the antibody and the isotype of IgG affect the ability of the antibody to harness effector mechanisms. For example, mouse IgGs are much less effective than human IgGs at mediating effector functions when tested *in vitro* using human effector cells and complement[27]. Mouse IgG2a and human IgG1 and IgG3 are the most effective at mediating ADCC, while mouse IgG3 and human IgG3 are the most effective at mediating CDC[28]. Studies have shown that human IgG1 is the isotype of choice for chimeric and humanized antibodies when the activation of effector mechanisms is desired[29].

*Advances in Monoclonal Antibody Engineering*

Early efforts in the clinical application of MAbs for cancer therapy were hampered by the immunogenicity, poor pharmacokinetics and suboptimal effector functions of mouse MAbs in humans. In the 1990s, advances in recombinant DNA technology led to the chimerization and humanization of MAbs to improve clinical efficacy[30]. Chimeric MAbs are

obtained by joining the antigen-binding variable domains of a mouse MAb to human constant region domains[27, 31]. Humanized MAbs are created by grafting the antigen-binding loops, or hypervariable regions, also known as complementarity-determining regions (CDRs), from a mouse MAb to a human IgG[32]. A previous study showed that the human anti-mouse antibody (HAMA) responses of mouse MAbs was dramatically reduced when MAbs were chimerized or humanized, and the HAMA responses between chimeric and humanized MAbs were similar[33]. In 1993, fully human antibodies were created in transgenic mice by introducing human antibody genes into mice lacking their own Ig loci[34]. The main advantage of this technology is that fully human MAbs from transgenic mice often have high affinity reflecting *in vivo* affinity maturation and thus obviate the need of *in vitro* affinity maturation. Although fully human MAbs are presumed to be less immunogenic than humanized or chimeric MAbs, there are no clinical data to substantiate this claim. This is not surprising since the idiotypes of both will be foreign to humans.

Antibodies can be engineered for enhanced anti-tumor activity. One way is to enhance their ADCC and CDC effector functions. As previously mentioned, the species of origin and the isotype of the MAb affect its ability to harness effector mechanisms. Therefore, chimerizing or humanizing MAbs to contain human Fc portions of the IgG1 or IgG3

isotype can potentially support these effector functions in humans. The importance of the Fc-FcγR interaction was first demonstrated in a study in which the potent anti-tumor activity of an anti-melanoma MAb was lost in mice that lacked FcγRI and FcγRIII[35]. ADCC is thought to be the mechanism underlying the antitumour effects of the Fc–Fcγ receptor interaction for this MAb. The importance of the Fc–Fcγ receptor interaction for antitumour activity was subsequently shown for both Rituxan™ and Herceptin™, an anti-Her2 MAb for the treatment of breast cancers[36]. The anti-tumor activity of Rituxan™ and Herceptin™ were greatly reduced in mice lacking the activating receptors FcγRI and FcγRIII. In contrast, their anti-tumor activity was enhanced in mice that lacked the inhibitory receptor FcγRIIB. These studies highlight the importance of the Fc–Fcγ receptor interaction for effector functions of MAbs. Advances in antibody engineering have exploited this to enhance the activity of several anti-tumor MAbs. For example, point mutations in the Fc region of an IgG1 have been made to increase in the binding affinity of the MAb to FcγRIII, resulting in a two-fold enhancement in ADCC *in vitro*[37]. Other studies have shown that interactions of MAb Fcs with effector cells are sensitive to changes in glycosylation and carbohydrate composition. Thus, changes have been made in the Fc region to enhance ADCC[38-40]. MAbs with improved CDC have been created by site-directed mutagenesis of the Fc

portion of the human IgG1. The mutant MAbs bound C1q more effectively[41].

Advances in antibody technology have also led to the production of multivalent MAbs, which are antibodies with more than two antigen-binding sites. Multivalent MAbs can be created by conjugating together two of the same IgGs by joining four identical variable regions to one Fc region, or by joining two pairs of variable regions each specific for a distinct epitope to a single Fc region to create a bispecific antibody. These multivalent MAbs were created to potentially improve the therapeutic efficacy of the MAb. The purported anti-tumor activity of tetravalent MAbs is the combination of secondary effector mechanisms (ADCC and CDC) and the induction of cell growth arrest and apoptosis by crosslinking surface antigens or by a decreased rate of dissociation from tumor cells. Multivalent MAbs have been made against CD20[42] and CD22[43], and have been tested preclinically with promising results.

Directly arming antibodies by covalent linkage to drugs, toxins or radionuclides is a widely explored strategy for enhancing the anti-tumor activity of antibodies. Armed antibodies typically show more potent anti-tumor activity in preclinical studies than their naked counterparts, although toxicity has remained a concern in clinical therapeutic use[16, 44]. Like naked antibodies, antibody conjugates are targeted to antigens found exclusively

on target cells or present at much lower levels on normal cells. However, a prerequisite for arming antibody with small molecule toxins, but not radionuclides, is that the antibody should be efficiently internalized. In contrast, because the β-particles of antibodies coupled to radionuclide span many cell diameters, bystander cells are often killed along with the targeted tumor cells. In contrast to naked MAbs, antibody conjugates should have shorter half-lives to reduce the risk of systemic toxicity.

*Antibodies for the Therapy of Hematological Cancers of B Cell Origins*

Rituxan™, Campath™, Bexxar™, Zevalin™ are all FDA approved MAbs or conjugated MAbs for the treatment of various hematological cancers of B cell origins such as NHL and chronic lymphocytic leukemia (CLL). Multiple MAbs are also being investigated preclinically and in clinical trials for potential anti-tumor activity against B cell lymphomas and leukemias. MAbs are being used as single agents or in combination with other MAbs with or without chemotherapy.

Rituxan™ was the first MAb to be approved by the FDA and has since been important in the treatment of diffuse large B-cell lymphoma, follicular lymphoma, and other types of NHL[45]. Rituxan™ is a chimeric IgG1 MAb that recognizes CD20, a transmembrane protein exclusively

expressed on mature B lymphocytes[46]. CD20 is expressed on most mature B cell malignancies but is not expressed on pro-B cells, pre-B cells, stem cells or plasma cells[47]. It is not shed into circulation and is not found in the plasma[47]. Rituxan™ is believed to mediate its activity primarily by ADCC and CDC of $CD20^+$ lymphoma cells, although other potential mechanisms of action have been demonstrated in pre-clinical studies[48, 49]. As a single agent, Rituxan™ induced remission in 48% of patients, and in combination with chemotherapy, Rituxan™ induced remission in 95% of patients[45]. The most common side effects associated with Rituxan™ are infusion related reactions such as fevers, chills, and rigors and immunosuppression-related infections due to a reduction in the number of B cells and other immune cells[45].

Bexxar™ and Zevalin™ are both radioconjugates that target CD20 on certain types of B cell NHL. Both have been approved for the treatment of Rituxan™-resistant relapsed, refractory indolent lymphomas. Bexxar™ is a murine IgG2aλ antibody labeled with $^{131}I$, and Zevalin™ is a murine IgG1κ antibody labeled with $^{90}Y$[50, 51]. Because these are radioconjugates and have a higher risk of toxicity than naked antibodies, both Bexxar™ and Zevalin™ are administered as a single course of treatment. The possible side effects of these therapeutic conjugates are prolonged and severe cytopenias, hypersensitivity including anaphylaxis, secondary

leukemias, hypothyroidism, and infusion-related toxicities such as fevers, chills, and rigors.

Campath™, also known as alemtuzumab, is a humanized IgG1κ MAb that recognizes CD52. CD52 is a surface peptide expressed in mature T and B lymphocytes, monocytes, macrophages, and some granulocytes. CD52 is strongly expressed in CLL and some indolent NHLs. Campath™ has been approved by the FDA for treatment of fludarabine-refractory CLL. Although it has been shown to induce apotosis and mediate CDC and ADCC against malignant lymphocytes *in vitro*, its exact mechanism of action has not yet been elucidated[52, 53]. In three separate studies, Campath™ has demonstrated 21-33% complete response rates in patients with B-CLL[54, 55] and is being evaluated in clinical trials in patients with a variety of other lymphoid malignancies[56]. Campath™ has been used as consolidation therapy after chemotherapy for CLL and has been proven effective[57, 58]. The most common adverse effects associated with Campath™ therapy are cytopenias, infusion reactions, myelosuppression, lymphopenia, and immunosuppression-related infection[54].

## C. CD19

*Structure*

CD19 is a 95 kDa transmembrane glycoprotein and a member of the Ig superfamily that is restricted to B cell expression in both mouse and humans[59]. The cytoplasmic region of CD19 is composed of approximately 240 amino acids[59] and contains nine conserved tyrosine residues, which is thought to mediate this region's interactions with the proto-oncogene Vav, phosphatidyl-inositol-3 (PI-3) kinase, and the Lyn, Lck, and Fyn protein tyrosine kinases[60-63]. The cytoplasmic region of human, mouse and guinea pig CD19 are highly homologous, which indicates the critical role of this region in the function of CD19[64, 65]. The CD19 extracellular region contains two C2-type Ig-like domains separated by a smaller potentially disulfide-linked domain[59]. On the surface of mature B cells CD19 forms a complex with Leu13, the tetraspan membrane protein TAPA-1 (CD81), and complement receptor 2 (CD21)[64, 66]. Together, these four molecules comprise the B cell co-receptor complex. They associate with the B cell receptor (BCR) complex to modulate signal transduction by the BCR[67].

*Expression on Normal Cells*

In both humans and mice, CD19 expression is restricted to B cells and is the most ubiquitously expressed membrane protein on the B cell lineage[68]. Of the variety of different surface antigens restricted to B lineage cells that include CD19, CD20, CD21, CD22, CD23, CD37, CD72 and membrane Ig, CD19 is the most widely expressed on normal B cells[69]. CD19 expression is absent in pluripotent $CD34^+$ hematopoietic stem cells, but CD19 is expressed upon commitment to the B lymphocyte lineage along with CD10. These progenitor B (pro B) cells lose their potential to differentiate into any other cell types and begin the rearrangement of the V regions of the μ heavy chain. Subsequently, these cells express the μ protein in the cytoplasm and CD22 on the cell surface at the pre-pre B cell stage. At this point, the V regions of the light chain begin to rearrange until a functional Ig is expressed on the surface of the immature B cell. CD20 expression occurs at approximately the same time as membrane Ig while CD10 expression is downregulated and only reappears again later in germinal center B cells following B cell activation. Most of the B lineage antigens are downregulated during terminal differentiation into plasma cells.

Thus, CD19 is expressed following the differentiation of the pluripotent stem cell into committed B lymphocytes, and its expression is not lost during subsequent stages of B cell differentiation until terminal differentiation into plasma cells. In addition, CD19 expression is limited exclusively to B lymphocytes, and it is not expressed on any other cell types.

*Functions*

*In vitro* studies suggest that CD19 signaling triggers a series of pleiotropic biochemical signals that lead to increased tyrosine phosphorylation of cytoplasmic and cell surface proteins, activation of phospholipase C, an increase in the concentration of free intracellular calcium ions ([$Ca^{2+}$]), stimulation of serine-specific protein kinases including protein kinase-C, and the activation of nuclear factor kappa-B (NFκB)[62, 70, 71]. These series of biological responses result in the modulation of B cell activation and growth regulation[70, 72, 73]. Signaling through CD19 is not dependent upon surface Ig expression since ligation of CD19 can provide proliferative signals for $IgM^-$ precursor B cells[62, 71].

Although CD19 plays a role in antigen-independent signaling responses, antigen-mediated signal transduction through the CD19

complex have important biological consequences. In one model of antigen-dependent CD19 function, CD21 bound complement-bound antigen and co-ligated CD19 (which is covalently bound to CD21) to the BCR[74]. In another model of antigen-dependent CD19 function, CD19 molecules were crosslinked by the binding of CD21 to complement-bound antigen. In both models, the results were amplification of BCR signaling, a decreased threshold of B cell activation, and the proliferation and differentiation of B cells into antibody producing cells[70, 75]. The CD19-BCR signaling complex therefore enables B cells to detect low concentrations of antigen. *In vivo* studies show that although there was normal generation and B cells in the bone marrow of CD19-deficient mice, there was a significant reduction in the numbers of B cells in the peripheral lymphoid tissues, and $CD19^-$ B cells exhibited a significantly decreased ability to proliferate in response to B cell mitogens such as lipopolysaccharide (LPS), anti-IgM antibodies, and CD40 ligation[76]. In contrast, over-expression of CD19 results in defective early B cell development in the bone marrow, augmented mitogenic responses, and increased serum Ig levels, which indicate that CD19 functions to define signaling thresholds for B cell selection, activation, and differentiation[76].

*Pathophysiology*

Surveys of large panels of B cell-lineage neoplasms indicate that CD19 expression is rarely lost during neoplastic transformation[77-80]. Therefore, CD19 is a useful marker in the diagnosis of B cell leukemias and lymphomas. CD19 is expressed in pre-B ALL, B-ALL, hairy cell leukemia, B-CLL, and NHL including Burkitt's lymphoma, but is not expressed on CML, AML, multiple myeloma (MM) or T-ALL[77]. The ability to phenotypically characterize leukemias and lymphomas has an important application in developing therapies since neoplastic hematologic cells are often present in a mixture of normal healthy cells. Therefore, anti-tumor therapies targeting the unique pattern of antigen expression identified on neoplastic cells will mitigate the undesired effects against normal peripheral blood or bone marrow cells. CD19 is a valuable marker in this regard since it is widely expressed within the B cell lineage, absent on all other cell types, and rarely lost during neoplastic transformation. Although targeting $CD19^{+}$ cells during immunotherapy will eliminate normal B lineage cells along with neoplastic B cells, differentiation of pluripotent stem cells can repopulate the B cell compartment following treatment since these cells are spared during anti-CD19 treatment.

In addition to being the most widely expressed cell surface antigen in the normal B cell lineage, CD19 also has the broadest expression of the B cell restricted antigens in the vast majority of B cell tumors based on the characterization of approximately 700 leukemias and lymphomas using MAbs against B cell lineage markers[81]. CD19 expression is positive in early B cell tumors including pre-B ALL even before surface Ig or CD20 expression. Although CD10 also appears in early B cell malignancies, its expression is low or lost in B cell lymphomas. Therefore, CD19 is the most ubiquitiously expressed normal and malignant B cell antigen. This has important implications for immunotherapy of B cell tumors. As previously discussed, the only FDA approved MAb therapies for tumors of B cell origin are CD20 or CD52-based immunotherapies such as Rituxan™, Zevalin™, Bexxar™ and Campath™. However, pre-B ALLs do not express CD20 or CD52, while other tumors can lose CD20 surface expression during the course of treatment[82-84]. Moreover, some patients do not respond to anti-CD20 or anti-CD52 therapy or relapse after treatment[85]. As compared to CD20, the expression of CD19 begins earlier and persists longer during B cell maturation. Consequently, the spectrum of lymphoid malignancies expressing CD19 is broader[81]. Therefore, CD19 is an attractive target for immunotherapies against early B cell malignancies such as pre-B ALLs, B cell tumors that have lost CD20

expression, and alternative regimens for patients who are refractory to anti-CD20 treatment.

**D. HD37**

*Naked Antibody*

An IgG1κ mouse anti-human CD19 MAb, HD37, has previously been developed and characterized for the treatment of B cell malignancies[86, 87]. With respect to normal hematopoietic cells, HD37 was found to be reactive against enriched B cell populations from peripheral blood mononuclear cells, but not against T cells, monocytes, granulocytes, erythrocytes, or platelets[86]. In the bone marrow population, HD37 was reactive against subpopulations of lymphoid, but not myeloid or erythroid cells. HD37 was also screened for reactivity against leukemic and lymphomic cell lines and was found to be reactive against NHL, B-ALL, B-CLL, and HCL, but not MM, T-CLL, or AML.

HD37 has anti-proliferative effects on B cell tumor lines *in vitro*. HD37 inhibited the growth of three $CD19^+$ Burkitt's lymphoma cell lines, Daudi, Namalwa, and Raji, and one $CD19^+$ diffuse histiocytic lymphoma cell line, DHL-4[87]. However, HD37 had no effect on the growth of $CD19^-$ T leukemia cell line, Jurkat. Therefore, the anti-proliferative activity of HD37 *in vitro* is specific for $CD19^+$ cell lines. Further *in vitro* studies suggest that the inhibitory effects of HD37 require the crosslinking of CD19 on the cell

surface[87, 88]. Crosslinking CD19 is thought to induce cell cycle arrest at $G_1$ and possibly $G_2$/M phases[87]. CD19 crosslinking is also thought to inhibit early activation of B cells, downregulate signaling, and block $Ca^{2+}$ influx in response to anti-Ig stimulation[88].

HD37 exhibits anti-tumor activity in severe combined immunodeficient (SCID) mice with human B cell tumor xenografts. In a previous study, HD37 prolonged the survival of SCID mice with Daudi tumors as determined by the mean paralysis time (MPT). Treatment with phosphate buffered saline (PBS) or isotype-matched control did not[87]. The anti-tumor activity of HD37 was dose-dependent, and it was well tolerated and prolonged the survival of the SCID/Daudi mice even at 5 mg, the highest dose tested. This dose, 5 mg per 20 g mouse, is equivalent to a human dose of 128 mg/$m^2$, which is at 34% of the single dose used for Rituxan™ treatment[45]. Therefore, *in vitro* and *in vivo* studies have demonstrated that HD37 may be an effective immunotherapy against B cell malignancies.

*Immunotoxin*

The anti-tumor efficacy of HD37 immunotoxins (ITs) has also been previously tested. HD37 was covalently conjugated to deglycosylated ricin

toxin A chain (dgRTA) to create the IT, HD37-dgRTA, which has been evaluated in both *in vitro* and *in vivo* studies for its cytotoxic effects against tumor cells. Previous *in vitro* studies have shown that HD37-dgRTA was effective in killing Burkitt's lymphoma cell lines (Daudi, Namalwa, and Raji), as well as a pre-B ALL cell line (NALM-6)[89, 90]. Further *in vivo* studies confirmed the anti-tumor activity of HD37-dgRTA either alone or in combination with an anti-CD22 IT and/or chemotherapy in SCID mice with human NHL or pre-B ALL[91-94]. HD37-dgRTA significantly extended the MST of SCID mice with human NHL or pre-B ALL compared to PBS and isotype-matched control IT, and the anti-tumor activity was further enhanced by combination therapy. In one study, the combination therapy of ITs against CD22 and CD19 as well as the chemotherapeutic drug, cytoxan, was curative in SCID mice with human NHL[93]. Cure was demonstrated by histopathologic examination and the adoptive transfer of cells from the ovaries and spinal cords of cured mice to healthy, naïve SCID mice.

The efficacy of immunotherapy with anti-CD19 ITs in patients was demonstrated in clinical trials using HD37-dgRTA alone or in combination with an anti-CD22-dgRTA[95-97]. These studies held promising results for the anti-tumor efficacy of the ITs although vascular leak syndrome is the major

toxicity. Approximately 25-30% of patients made antibodies against mouse Ig (HAMA) or dgRTA but could be retreated when antibody titers dropped.

*Homodimer*

Since previous reports have suggested that HD37 can signal cell cycle arrest and/or apoptosis by inducing negative cell signaling[87, 88], HD37 was chemically conjugated into a homodimer consisting of two IgG molecules covalently coupled together with a thioester bond[98]. Homodimers are large tetravalent antibody molecules thought to efficiently crosslink their targets. HD37 homodimers had anti-growth activity on target Daudi cells whereas the monomers had no effect even at $10^{-6}$ M, the highest concentration tested. The homodimers, but not monomers, arrested Daudi cells at the $G_0/G_1$ cell cycle phase, and the homodimers were found to have a slower dissociation rate from cells than monomers. In addition, *in vivo* tests showed that the HD37 homodimers significantly extended the MST of SCID mice with Daudi tumors compared to monomers. Therefore, dimerizing HD37 increased its potency presumably by increased negative signaling due to hypercrosslinking and/or a slower dissociation rate compared to monomeric HD37. However, the effector functions of the homodimers were not evaluated.

**E. Summary and Study Objectives**

Although MAbs have become an important treatment option for the therapy of many cancers due to their specific targeting ability and their relatively low systemic toxicity compared to traditional cancer treatments such as chemotherapy, there is currently no FDA-approved MAb for the treatment of pre-B ALLs, which affect thousands of children and adults in the U.S. every year. CD19 is an attractive target for MAb therapy because it is a pan-B cell marker that is expressed on both normal and neoplastic B cells early in B cell development at the pre-B cell stage and is not expressed on any other cell types. Furthermore, it is expressed before CD20, another B cell restricted antigen expressed on mature B cells and is the target for Rituxan™, which is the only FDA-approved MAb therapy for B cell specific tumors. HD37 is a mouse anti-human CD19 IgG1 MAb and has promising anti-tumor activity against B cell malignancies including pre-B ALL and NHL in both mice and humans. HD37 was also dimerized to create a large antibody molecule, which was shown to have better anti-tumor activity than the monomer presumably due to hypercrosslinking of CD19 on their target cells and/or a slower dissociation rate from the cell surface. However, mouse antibodies in humans often elicit an HAMA response, thereby decreasing the anti-tumor efficacy of the therapeutic

MAb. Moreover, the clinical use of the HD37 homodimer is limited due to its large size and limited effector functions. The latter is important for its mechanism of action.

Therefore, the objectives of this study were to construct, express, and test the *in vitro* and *in vivo* activities of both divalent and tetravalent forms of chimeric HD37 MAbs with the goal of using these data to determine which chimeric HD37 to move forward into clinical trials. Chimeric MAbs, which are antibodies with human constant regions and mouse variable regions, are far less immunogenic than their mouse counterparts and can efficiently carry out effector functions in humans due to their ability to engage human effector cells and complement with their Fc regions. Tetravalent MAbs, which are antibodies with one human Fc and four mouse variable regions, are smaller in size than their homodimeric counterparts and can carry out normal effector functions. The activities of the two cHD37 MAbs (divalent and tetravalent) were compared to each other as well as to the murine HD37.

# CHAPTER TWO

## Materials and Methods

### A. Construction, Expression and Purification of the Chimeric MAbs

*Construction of cHD37*

The heavy and light chains of cHD37 were generated using vectors containing the human IgG1 and kappa constant domains, pAH4604 and pAG4622, a generous gift from Dr. Sherie Morrison[99]. The heavy and light variable domain sequences of HD37 have been reported previously[100]. These domains were separately amplified by polymerase chain reaction (PCR) from cDNA prepared from HD37-secreting hybridoma cells using primers that anneal in their respective inferred leader peptides and the constant domains. The primers, designated A through D, including additional flanking restriction sites (underlined), are as follows: A (heavy chain leader), 5' – GGGTCTAGATATCCACCAT GGGATGGAGCTTGATCTTTCTCTT – 3'; B (heavy chain constant), 5' – AGGGAATTCA(C/T)CTCCACACACAGG(A/G)(A/G)CCAGTGGATAGAC – 3'; C (light chain leader), 5' – GGGTCTAGATATCCACCATGGAGAC

AGACACACTCCTGCTATGGG – 3'; and D (light chain constant), 5' – GCGGAATTCGCTCACTGGATGGTGGGAAGATGGA – 3'.

PCR products were separately cloned into pUC18 using *Xba*I and *Eco*RI restriction sites, and the variable domain sequences were verified by DNA sequencing. Primers A and C were then used in conjunction with their corresponding 3' primers E and F, respectively, to amplify HD37 genes for inserting into the two heavy chain and light chain antibody vectors. The sequences for the 3' primers are: primer E (heavy chain 3' – end), 5' – GTCTAGGAATTCGCTAGCTGAGGAGACGGT GACTGAGG – 3'; and primer F (light chain 3' – end), 5' – GTCTAGGAATTCGTCGACTTACGTTTGATTTCCAGCTTGGTGC – 3'. The heavy chain vector and heavy chain variable domain were digested with *Nhe*I and *Eco*RV restriction enzymes for ligation while *Sal*I and *Eco*RV were used for the light chain vector and variable region.

The heavy and light chain constructs were co-transfected into non-secreting murine myeloma SP2/0 cells (ATCC, Manassas, VA) using Lipofectamine 2000 (Invitrogen, Carlsbad, CA). 2 X $10^6$ SP2/0 cells/well grown in complete medium containing Dulbecco's Modified Eagle's Medium (DMEM) (Sigma, St. Louis, MO) supplemented with 10% heat inactivated (45 min incubation at 56°C) fetal bovine serum (FBS) (Hyclone, Logan, UT), 2 mM L-glutamine (Sigma, St. Louis, MO), were

plated in a 6-well plate. Lipofectamine complexed with heavy chain or light chain plasmids was added drop-wise to the plated cells. The Lipofectamine-DNA complexes were prepared by adding 0, 2, 4, 6, 8, or 10 µg HD37 heavy or light chain plasmids to 250 µl Opti-MEM solution (Invitrogen, Carlsbad, CA) and 10 µl Lipofectamine 2000. Following 24 hr incubation, cells were transferred to 96-well plates at a density of ~ 1.67 X $10^4$ cells/well, and cells were again incubated for another 24 hr. Stable transfectants were selected by adding L-histidinol (Sigma, St. Louis, MO) to the wells at a final concentration of 5 mM. Medium in the wells was replaced with fresh medium containing drug every 72 hr until cells grew to ~ 80 – 90% confluency, as determined by visualization through a light microscrope under 10X magnification (Olympus, Dexter Co., San Antonio, TX). Supernatants from these wells were then screened using an enzyme linked immunosorbent assay (ELISA) to identify wells with antibodies secreted by the cells.

Cells secreting > 2.5 mg/L antibody were then subcloned at 1 cell/well to obtain monoclonal cell populations. Cells were sequentially diluted in complete medium containing 5 mM L-histidinol to a concentration of 5 cells/mL. Diluted cell suspensions were then plated in 20 96-well tissue culture plates (such that the average number of cells per well is 1) and incubated at 37°C and 5% $CO_2$. 100 µL of the media was

carefully pipetted out from the top of the wells without disturbing the cells every 72 hr and replaced with fresh complete media containing 5 mM L-histidinol until cells grew to ~ 80 – 90% confluency, as determined by visualization through a light microscrope under 10X magnification. Supernatants from these wells were then screened for antibody production by ELISA. Seven monoclonal populations with the highest antibody secretion were selected for expansion. Cells were transferred from the 96-well plates to 24-well plates, 6-well plates, 75 $cm^2$ tissue culture flasks and 175 $cm^2$ tissue culture flasks successively each time confluency reached to ~ 80 – 90%. Cells were then centrifuged at 300 x *g* for 10 mins at 4°C (Kendro Laboratories, Model RC3C, Waltham, MA) and resuspended in freezing medium containing 92% heat inactivated FBS and 8% DMSO (Sigma, St. Louis, MO). Cells were stored in cryogenic storage vials (Corning, Lowell, MA) at $10^7$ cells/mL/vial overnight at -80°C and transferred to -140°C Harris Cryostar freezer (Kendro Laboratories, Waltham, MA) the next day for long-term storage.

*Construction of cHD37-DcVV*

cHD37-DcVV was constructed by building additional variable domains into the divalent cHD37. In this construct, the heavy chain

variable region (VH) gene of the divalent cHD37 was replaced with a gene encoding VH-SGGGGS-VH, while the light chain variable region (VL) gene was substituted with VL-SGGGGS-VL. HD37 VH was modified by PCR using the following primers designated G through J (the restriction sites are underlined): G, 5' – GTCGAGAATTCCTCGAGCACCATGGG ATGGTCATGTATC – 3'; H, 5' – CTAGATATATTCCGGATGAGGAAA CGGTGACTGAGG – 3'; I, 5' – CTAGATATATTCCGGAGGTGGAGGTT CACAGGTTCAGCTGCAGCAGTC – 3'; and J, 5' – GTCTAGGAATT CGCTAGCTGAGGAGACGGTGACTGAGG – 3'. The PCR products of VH domain were then digested with *Xho*I/*Bsp*EI and *Bsp*EI/*Nhe*I restriction enzymes and inserted in-frame by three-way ligation into the di-cistronic pIZDHL vector (Xiao-yun Liu & Ellen S. Vitetta, unpublished data), which was digested with *Xho*I/*Nhe*I, to create the pIZDHL-VVH37 plasmid. HD37 VL domain was modified by PCR using the following primers designated K through N (the restriction sites are underlined): K, 5' – CTAGATATATACGCGTCACCATGGAGACAGACACACTCCTG – 3'; L, 5' – CTATATATATTCCGGATTTGATTTCCAGCTTGGTGCC – 3'; M, 5' – CTAGATATATTCCGGAGGAGGAGGTTCAGACATTGTGCTGACCCAAT C – 3'; and N, 5' – GAACCTGTGCAGCCACCGTACGTTTGATTT CCAGCTTGGTGCC – 3'. The PCR products of VL were then digested with *Mlu*I/*Bsp*EI and *Bsp*EI/*Bsi*WI and inserted in-frame by three-way

ligation into the pIZDHL-VVH37 plasmid digested with *Mlu*I/*Bsi*WI to create the pcHD37-DcVV plasmid.

The pcHD37-DcVV plasmid was then transfected into CHO/DHFR$^-$ cells using Lipofectamine™ LTX (Invitrogen, Carlsbad, CA) using the same method described previously for the cHD37 plasmid transfection. Cells were cultured in complete medium containing Iscove's Modified Dulbecco's Media (IMDM) (Sigma, St. Louis, MO) supplemented with 10% dialyzed FBS. Stable transfectants were selected in complete media containing 200 µg/mL Zeocin (Invitrogen, Carlsbad, CA). Antibody expression levels were determined by ELISA.

*ELISA*

When cells from the transfection experiments were at ~ 80 – 90% confluency, cells would be prepared for ELISA to determine the level of antibody expression. Cells were resuspended by gentle pipetting, and replated in a well of a 24-well tissue culture plate with fresh complete medium containing drug (cHD37: DMEM + 10% heat inactivated FBS + 2 mM L-glutamine + 5 mM L-histidinol; cHD37-DcVV: IMDM + 10% dialyzed FBS + 200 µg/mL Zeocin). Cells were incubated at 37°C and 5% $CO_2$ until ~ 80 – 90% confluency. Viability and number of cells were determined by

Trypan Blue (Invitrogen, Carlsbad, CA) exclusion. Cells were transferred from the well to a sterile microcentrifuge tube, centrifuged at 300 x *g,* and resuspended to a density of 2 X $10^5$ cells/mL in fresh medium containing drug. One mL of cells were then transferred to a well in a new 24-well plate and incubated for 96 hr at 37°C and 5% $CO_2$. Following incubation, the supernatant was collected for immediate analysis of antibody production.

96-well, high binding ELISA plates (BD Bioscience, San Jose, CA) were coated with goat anti-human IgG γ-chain specific antibody (Sigma, St. Louis, MO) at a concentration of 10 µg/mL and incubated overnight at 4°C. Plates were washed with PBS + 0.05% Tween-20 (Sigma, St. Louis, MO) buffer. A multi-channel pipet was used to dispense 250 µL of the buffer into each well. The plate was inverted over the sink, flicked to eliminate fluid, and blotted on clean paper towels. This washing procedure was repeated until the plate had been washed a total of three times. 200 µL of blocking buffer containing 1X PBS + 2% BSA + 0.05% $NaN_3$ (Sigma, St. Louis, MO) was added to each well of the plates. Plates were then incubated overnight at 4°C. The next day, plates were washed ten times with $dH_2O$.

The standard, chimeric anti-CD54 MAb, cUV3[101], was diluted to 1 µg/mL in dilution buffer containing 1X PBS + 0.5% bovine serum albumin

(BSA) (Sigma, St. Louis, MO) + 0.0125% $NaN_3$, and six 2-fold serial dilutions were prepared from this initial concentration. Supernatants from the cells that had been incubated for 96 hr were diluted to an initial concentration of 1:5 with dilution buffer, and six 2-fold serial dilutions were also prepared. Fifty microliters of each standard and supernatant dilution were added in triplicate to the respective wells of a 96 well plate pre-coated with the goat anti-human IgG γ-chain specific antibody. Plates were wrapped in plastic wrap and incubated for 1 hr at 37°C.

Following incubation, plates were developed. Plates were washed ten times with $dH_2O$. Fifty microliters of goat anti-human Fc-specific IgG-alkaline phosphatase conjugated antibody (Sigma, St. Louis, MO) diluted in blocking buffer was added to each well. Plates were wrapped in plastic wrap and incubated for 1 hr at 37°C and washed ten times with $dH_2O$. Each well then received 50 μL substrate solution composed of p-Nitrophenyl phosphate disodium salt hexahydrate (p-NPP) dissolved in 1.5 mL 0.1 M $Na_2CO_3$ + 1.0 mL 0.1 M $NaHCO_3$ + 2.5 mL $dH_2O$. The color of the sample was measured at 492 nm using a Molecular Devices ThermoMax microplate reader. The amount of antibody present in unknown samples from the cell supernatant was calculated from the standard curve where known concentrations of cUV3 were used.

*Expression and Purification of the Chimeric MAbs*

MAb secreting cell clones were grown in 175 $cm^2$ tissue culture flasks in complete medium containing DMEM (for cHD37) or IMDM (for cHD37-DcVV) supplemented with 10% heat inactivated IgG-free FBS, 4 mM L-glutamine, 100 units/ml penicillin and 100 μg/ml streptomycin (Invitrogen, Carlsbad, CA). Heat inactivated IgG-free FBS was prepared by protein G-sepharose (Amersham Biosciences, Piscataway, NJ) affinity purification. FBS was first inactivated at 56°C for 45 min. After cooling to room temperature, FBS was passed through a 25 mL protein G-sepharose column, previously equilibriated with pH 7.4 PBS, at 4°C at a rate of 3 mL/min. The flow through was collected, and the column was cleaned with 200 mL 0.1 mol/L glycine-HCl-$NaN_3$ buffer, pH 2.8, and then equilibriated with PBS, pH 7.4. The eluted FBS was passed through the column once more, and the final eluted product was filtered through 0.22 μm vacuum filters to sterilize the purified, IgG-free FBS. Bovine IgG contaminant was checked with Ouchterlony (The Binding Site, Birmingham, UK). 10 μL of the purified FBS was added to a well of the Ouchterlony gel plate. 10 μL of goat anti-bovine IgG antibody (Sigma, St. Louis, MO) was added to the adjacent well on the plate. The presence of a band (precipitation) between the wells after 24 hr of incubation at room temperature indicates that

bovine IgG is still present in the purified FBS. Only FBS that does not precipitate in the presence of goat anti-bovine IgG antibody is considered “IgG-free”.

Once the cells reached ~80 – 90% confluency, the cells were transferred to two liter capacity roller bottles (BD Falcon, Bedford, MA and Corning) supplemented with up to 1.2 L complete media. The roller bottles were gassed for 36 hr with loose caps at 37°C, 5% $CO_2$. The roller bottles were then tightly capped and moved to a roller cabinet (Bellco Biotechnology, Vineland, NJ) rotating at 1.5 rpm.

When cell viability was < 20% as determined by Trypan Blue exclusion, the cell suspension was centrifuged at 4°C, 1850 x g for 30 min to separate the hybridoma cells from the supernatant containing the antibody. The supernatant was collected, and 300 g/L ammonium sulfate (Sigma, St. Louis, MO) was added to the supernatant for 24 hours at 4°C to precipitate the proteins. The mixture was centrifuged at 1850 x *g* for 30 min at 4°C, and the supernatant was discarded. The precipitate was dissolved in a small volume of distilled water until the solution was transparent, and the dissolved solution was dialyzed overnight against PBS, pH 7.4. The dialysate was filtered through a 0.22 µm filter and passed through an affinity-purified 5 mL protein G-sepharose column previously equilibriated with PBS, pH 7.4, at a rate of 3 mL/min. The MAb

was then eluted with 0.1 M Glycine-HCl-$NaN_3$ buffer, pH 2.8, until all the MAb had been eluted. The eluate was collected in 1 mL fractions in 12 x 75 mm borosilicate glass tubes (Kimble Glass Inc., Vineland, NJ) filled with 200 µL of 1.0 M Tris-HCl, pH 8.0 (Sigma, St. Louis, MO) to neutralize the acidity of the antibody solution. A fraction collector was connected to a recorder and ultraviolet sensor (LKB Bromma, Bromma, Sweden) used to monitor antibody elution. Based on the recorder chart, selected fractions were further analyzed by measuring their absorbance in a separate Beckman-Coulter DU-640 spectrophotometer (Fullerton, CA), and elution was stopped when the $OD_{280}$ was less than 0.05. Fractions with an $OD_{280}$ absorbance reading greater than 0.05 were pooled. The amount of protein collected was determined by spectrophotometry, and the antibody solution was dialyzed overnight at 4°C in PBS, pH 7.4. The dialysate was concentrated to 1.0 mg/mL, filter-sterilized, and stored at 4°C.

*Sodium Dodecyl Sulfate Polyacrylamide Gel Electrophoresis (SDS-PAGE) Analysis*

The purity of the MAb was analyzed by 4-15% SDS-PAGE using the PhastGel system (Amersham Biosciences, Piscataway, NJ). An equal volume of the antibody sample at a concentration of 1 mg/mL was

combined with either reducing buffer (1.25 mL 1.0 M Tris-HCl at pH 6.8, 4 mL 10% SDS, 1 mL 2-mercaptoethanol, 2 mL glycerol, 1.25 mL distilled water, 0.5 mL 0.1% Bromophenol Blue) or non-reducing buffer (reducing buffer without 2-mercaptoethanol), and the sample was then placed in a heat block (Lab-Line Instruments, Dubuque, IA) at 100°C for 3 min. Three microliters of the sample was loaded by capillary action into the teeth of the loading comb and transferred to the comb slot in the gel holder. Samples were electrophoresed on a continuous 4-15% gradient PhastGel (Amersham Biosciences, Piscataway, NJ) with SDS buffer strips (Amersham Biosciences, Piscataway, NJ) inside the separation unit for approximately 30 min, until the voltage reached 65V. The gel was then stained by Coomassie Blue [50% prepared Blue R dye (Amersham Biosciences) and 10% acetic acid] and de-stained with a solution of 10% acetic acid and 30% methanol in distilled water according to set developer programming (5, 8, and 10 min washes).

## B. Culture of Human Cell Lines

*Culture of Human Tumor Cell Lines*

All human tumor cell lines were obtained from the American Type Culture Collection (ATCC) (Manassas, VA) including the $CD19^+$ human Burkitt's lymphoma cell lines Daudi, Namalwa, and Raji; and the $CCD19^+$ human precursor B cell acute lymphoblastic leukemia cell line NALM-6. Cells were maintained in culture by serial passages in complete medium containing Roswell Park Memorial Institute-1640 (RPMI-1640) media (Sigma, St. Louis, MO) supplemented with 10% heat-inactivated FBS containing 2 mM L-glutamine, 100 units/ml penicillin and 100 µg/ml streptomycin. The cells were grown in a humidified atmosphere of 5% $CO_2$ at 37°C. Cell viability was determined by Trypan Blue exclusion.

For freezing, cells were centrifuged at 300 x *g* for 10 min at 4°C and resuspended in freezing medium containing 92% heat inactivated FBS and 8% DMSO. Cells were stored in cryogenic storage vials at $10^7$ cells/mL/vial overnight at -80°C and transferred to -140°C the next day for long-term storage.

*U937 Cells*

The human FcγRI/III$^{+}$CD19$^{-}$ human leukemic monocytic lymphoma cell line, U937, was also obtained from ATCC. Cells were maintained in culture by serial passages in complete medium containing RPMI-1640 media supplemented with 10% heat-inactivated FBS containing 2 mM L-glutamine, 100 units/ml penicillin and 100 µg/ml streptomycin. The cells were grown in a humidified atmosphere of 5% $CO_2$ at 37°C. Cell viability was determined by Trypan Blue exclusion. Cell freezing was performed in the same manner as the human tumor cell lines.

*Isolation and Culture of Normal Human B Cells*

Normal human B cells were obtained from healthy donors under informed consent and approved by the Institutional Review Board committee of the University of Texas Southwestern Medical Center. Peripheral blood mononuclear cells (PBMCs) were isolated by density gradient centrifugation. Whole blood was drawn from donors using 21 ¾ G butterfly needles and into Vacutainer tubes containing anticoagulant ACD solution (BD Bioscience, San Jose, CA). Up to 20 mL of whole blood was

transferred to 50 mL polypropylene centrifuge tubes (BD Bioscience, San Jose, CA) and mixed with an equal amount of sterile PBS, pH 7.4. Fourteen milliliters of Histopaque-1077 (Sigma, St. Louis, MO) was layered on the bottom of the PBS-whole blood mixture using a 14 mL pipette. Cells were centrifuged at 300 x *g* for 30 min at room temperature with the centrifuge brakes off. The PBMC layer at the plasma/Histopaque interface was isolated and washed three times with PBS, pH 7.4 by centrifugation at 300 x *g* for 10 min at room temperature. PBMCs were then resuspended to $10^7$ cells per 40 µL buffer containing PBS at pH 7.4, 2 mM EDTA (Sigma, St. Louis, MO) and 0.5% heat inactivated FBS. Cell viability and number was assessed by Trypan Blue exclusion.

Immunomagnetic negative selection of human B cells from PBMCs was performed with a B-cell isolation kit (Miltenyi, Auburn, Calif.), according to the manufacturer's instructions. PBMCs were incubated for 10 min at 4°C with 10 µL of biotin-antibody cocktail (provided in the kit) per $10^7$ cells. The cocktail is a mixture of biotin-conjugated MAbs against CD2 (T and NK cells), CD14 (macrophages and neutrophils), CD16 (NK cells, neutrophiles, monocytes, and macrophages), CD36 (monocytes and platelets), CD43 (T cells, monocytes and granulocytes), and CD235a (erythrocytes). Following incubation, 30 µL of buffer and 20 µl of anti-biotin microbeads (provided in the kit) were added per $10^7$ cells, and cells were

incubated for additional 15 min at 4°C. Cells were then washed with 2 mL buffer per $10^7$ cells, centrifuged at 300 x *g* for 10 min at room temperature and resuspended at concentrations up to $10^8$ cells in 500 µL of buffer. MACS® separation columns, size LS, (one column per $10^8$ labeled cells) (Miltenyi, Auburn, CA) equilibriated three times with 3 mL cold buffer, were placed in the magnetic field of a MiniMACS® magnetic separator (Miltenyi, Auburn, CA). The cell suspension was applied to the column by pipetting. The cells that passed through the column were collected. The column was washed three times with buffer, and the eluate was also collected. Cell viabilities and numbers were determined by Trypan Blue exclusion. The purity of the negatively selected B cells was determined by flow cytometry. Negatively selected B cells were stained with fluorescein isothiocyanate (FITC) (BD Bioscience, San Jose, CA) coupled mouse anti-human CD19 and propidium iodide (PI) (BD Bioscience, San Jose, CA). Four-color flow cytometry was performed on a FACSCalibur (BD Bioscience, San Jose, CA), and analyzed with Cellquest software (BD Bioscience, San Jose, CA). The purity of negatively selected B cells was 90 - 95%.

**C. Cell Surface Staining and Flow Cytometry**

Human cell lines were washed twice with PBS, pH 7.4, and resuspended to $10^6$ cells per 100 µL in 12 x 75 mm polystyrene tube (BD Bioscience, San Jose, CA). Cells were then incubated with dilutions of MAbs (0.01 – 10 µg/mL) for 30 min at 4°C. Cells were washed three times with PBS, and resuspended to a volume of 100 µL of PBS. Goat anti-human Ig or goat anti-mouse Ig antibody coupled to FITC (BD Bioscience, San Jose, CA) were added to the cells under saturating conditions (as determine by prior titration). Cells were incubated for another 30 min at 4°C followed by three washes with PBS. Cells were resuspended to 250 µL PBS and maintained on ice prior to analysis by flow cytometry. In some experiments, the primary antibody was coupled to a fluorphore, and only one incubation was required.

Data were acquired using a FACscaliber (BD Biosciences, Bedford, MA) and analyzed using CellQuest software (BD Biosciences). Only live cells were analyzed, and the positive cut-off for the FITC channel was set so that no more than 5% of the negative control cells were considered positive. The percentage of positive cells was plotted against the MAb concentration.

**D. Binding Affinity and Dissociation of MAbs**

*Radiolabeling of the MAbs*

MAbs were radiolabeled with $Na^{125}I$ (Amersham Biosciences, Piscataway, NJ) using Iodogen reagents as previously described[102]. The free $Na^{125}I$ was removed by centrifugation on MicroSpin G-25 columns (Amersham Biosciences, Piscataway, NJ). The specific radioactivity of the labeled proteins was in the range of 4-8 x $10^6$ cpm/µg with < 5.5 % free $Na^{125}I$.

*Relative Binding Affinity of MAbs to NALM-6 and Daudi Cells*

NALM-6 or Daudi cells were suspended in complete medium at $10^7$ cells/mL and incubated with different concentrations of radiolabeled MAbs (0.25 – 4 µg/$10^7$ cells/mL) for 60 min at 4°C. Cells were then washed in RPMI-1640 media and centrifuged at 300 x *g* for 10 min at 4°C three times. Cells were resuspended in complete medium at $10^7$ cells/mL. Four aliquots of 100 µL cell suspension were applied to 400 µL mixture of phthalic acid/phthalate oil (Sigma, St Louis, MO) in microcentrifuge tubes (VWR Scientific, Suwanee, GA) and centrifuged. The tubes were frozen at

–80°C, and the tips of the test tubes were cut off. The radioactivity in both the tip (cell-bound radioactivity) and the remainder of the tube (free radioactivity) were measured. The binding curves represent the amount of protein added (in µg/$10^7$cells/mL) *versus* the amount bound (ng/$10^7$ cells). Scatchard plots were generated, and the binding constants ($K_a$) were calculated as previously described[103].

*Dissociation of MAbs from NALM-6 and Daudi Cells*

NALM-6 or Daudi cells were suspended in complete medium at $10^7$ cells/mL and incubated with 5 µg/mL of the radiolabeled MAbs for 60 min at 4°C. Cells were then washed in cold complete media and centrifuged at 300 x *g* for 10 min at 4°C three times and resuspended in 1 mL cold media. Unlabeled MAb was added to the cell suspension at a final concentration of 1 mg/mL, and the cells were incubated in 5% $CO_2$ at 37°C for 0 – 90 min in 30 min intervals**.** The dissociation of the radiolabeled MAbs was measured in the presence and absence of cold MAb. At each interval of time, triplicate aliquots of 100 µL were removed and centrifuged, and the radioactivity of the pellet and supernatant was measured. The results were expressed as the percentage reduction of the bound radioactivity *versus* time.

**E. Cell Proliferation**

*[$^3$H]Thymidine Incorporation Assay*

Human tumor cell lines in complete medium were cultured at a density of 5 X $10^4$ cells per well in flat bottomed 96-well plates and incubated for 72 hr in 5% $CO_2$ at 37°C with different concentrations of MAb ($10^{-6}$ to $10^{-9}$ M). After incubation, the plates were pulsed for 4 hr with 0.5 µCi of [$^3$H]thymidine (Amersham Biosciences, Piscataway, NJ). Cells were collected onto FilterMAT harvester paper (Skatron Instruments, Sterling, VA) using a cell harvester (Skatron Instruments). The filter paper was air dried and the perforated circles on the filter paper were placed into individual scintillation vials (Research Products, Mount Prospect, IL). CytoScint scintillation fluid (MP Biomedicals, Solon, OH) was added to each vial in a volume of 2 mL. CytoScint scintillation fluid (MP Biomedicals, Solon, OH) was added to each vial in a volume of 2 mL. The percentage reduction in [$^3$H]thymidine incorporation *versus* the concentration of MAbs was used to quantitate the cytotoxic effect of the MAbs (expressed in $IC_{50}$, defined by the concentration of MAbs which kill 50% of cells compared to control).

*Cellular Metabolism of a Tetrazolium Compound*

Human tumor cell lines in complete medium were cultured at a density of 5 X $10^4$ cells per well in flat bottomed 96-well plates and incubated for 72 hr in 5% $CO_2$ at 37°C with different concentrations of MAb ($10^{-6}$ to $10^{-9}$ M). After incubation, CellTiter 96® $AQ_{ueous}$ One Solution Reagent (Promega, Madison, WI) was added to each well according to the manufacturer's instructions and incubated for another 4 hr. The $AQ_{ueous}$ One reagent contains a tetrazolium compound and an electron coupling agent, which is reduced to a formazan product by healthy cells. The formazan product can be measured colorimetrically, which corresponds to the relative number of viable cells present. Data were obtained by scanning the plate with a Tecan Spectafluor Plus plate reader (Maennedorf, Switzerland) set at a wavelength of 490 nm. The data was analyzed with Magellan 2 software (Tecan). After 4 hr in culture, cell viability was determined by measuring the absorbance at 490 nm. The percent viability *versus* the concentration of MAbs was used to quantitate the cytotoxic effect (expressed as an $IC_{50}$).

## F. Antibody Dependent Cellular Cytotoxicity (ADCC)

*Preparation of Human Natural Killer Effector Cells*

NK cells were obtained from healthy donors with informed consent using the RosetteSep NK cell enrichment mixture (StemCell Technologies, Vancouver, Canada) as recommended by the manufacturer. Briefly, whole blood from donors was collected in Vacutainer tubes with ACD anti-coagulant solution. Whole blood was mixed with an equal volume of buffer containing PBS + 2.5% heat inactivated FBS in a 50 mL centrifuge tube. An equal amount of RosetteSep™ DM-L density separation media (StemCell Technologies) was layered on top of the mixture. The tube was centrifuged at 300 x *g* for 20 min at room temperature. The enriched NK cells were collected from the density separation media/plasma interface and washed three times with buffer. Cell viability was determined by Trypan Blue exclusion. Cells were resuspended to a density of $5 \times 10^6$ cells/mL in complete culture medium containing RPMI-1640 supplemented with 10% heat inactivated FBS. The purity of the NK cell population was determined by flow cytometry. NK cells were stained with FITC-conjugated mouse anti-human CD56 (BD Bioscience, San Jose, CA), a cell surface antigen whose

expression is limited to NK cells, and propidium iodine (BD Bioscience, San Jose, CA). Four-color flow cytometry was carried out on a FACSCalibur and analyzed with Cellquest software. The purity of human NK cells was 60 - 85%.

*Preparation of Murine Lymphokine-Activated Killer (LAK) Effector Cells*

Murine LAK cells, consisting primarily of mouse NK cells, T cells, B cells, and monocytes, were obtained from the spleens of 8 – 10 week-old Swiss Webster mice (Taconic Farms, Germantown, NY) using the MACs NK Cell Isolation Kit (Miltenyi, Auburn, CA), as recommended by the manufacturer. Briefly, mice were sacrificed by $CO_2$ asphyxiation according to UTSW institutional policy. The spleens were removed and placed into 30 mL of sterile Hank's balanced salt solution (HBSS; Sigma-Aldrich). The spleens were sliced into sections using sterile procedure and homogenized using two frosted glass slides. The cell suspension was passed through a sterile 70 µm cell strainer to remove tissue debris and then centrifuged at room temperature at 300 x *g* for 10 min. The supernatant was discarded, and the cell pellet was resuspended in 4 mL of M-lyse buffer from the Mouse Erythrocyte Lysing Kit (R & D Systems, Minneapolis, MN) and incubated at room temperature for 10 min. The lysis

reaction was stopped with 25 mL of PBS containing 2% FBS, and the cells were washed and centrifuged three times at 200 x *g* for 10 min at room temperature with PBS. The cells were resuspended to a concentration of 1.2 X $10^5$ cells/mL in complete medium containing DMEM supplemented with 10% heat inactivated FBS, 2 mM L-glutamine, 100 units/ml penicillin and 100 μg/ml streptomycin, 20,000 IU/mL recombinant human IL-2 (Roche, Emeryville, CA), 5.6 mM beta-mercaptoethanol (BME) (Sigma), and 0.5 μL/mL indomethacin (Sigma). Cells were incubated for 5 days for full activation. After incubation, cells were washed three times and resuspended to 5 x $10^6$ cells/mL in RPMI-1640 + 10% heat inactivated FBS.

*Preparation of Target Cells*

NALM-6 or Daudi cells were centrifuged at 300 x *g* for 10 minutes at 4˚C and resuspended to $10^7$ cells/mL in RPMI-1640. Cell viability was determined by Trypan Blue exclusion. A cell suspension volume of 500 μL was mixed with 150 μL $^{51}$Chromium stock (1 mCi/mL; Amersham Biosciences) and incubated for 1 hr at 37˚C in the dark with mixing every 15 min to enhance labeling. After an hour, the cells were washed twice in RPMI-1640. Cells were resuspended in 100 μL RPMI-

1640, and 5 µg of was antibody added to the cells. Cells were incubated at 37˚C for 30 min in the dark with mixing after 15 min. The cells were washed twice in RPMI-1640 and resuspended to 5 x $10^4$ cells/mL in RPMI-1640/10% heat inactivated FBS.

*$^{51}$Chromium Release Assay*

The cytotoxicity assay was performed as previously described[104]. Complete medium containing 2% Triton X-100 (Sigma, St Louis, MO) was used as a positive control to determine maximum $^{51}$Cr release. The effector to target ratios (E:T) were 100:1, 50:1 and 10:1. Effector cells were diluted accordingly to achieve the appropriate E:T ratio, and 100 µL of each of the prepared effector and target cells were mixed together and added in triplicate in 96-well plates. The plates were incubated at 37°C for 6 or 18 hr. The plates were then centrifuged, and the amount of radioactivity in the cell supernatant from each well was determined using a gamma counter (Wallac Wizard, PerkinElmer, Wellesley, MA). Specific lysis was calculated using the following equation: Specific percent lysis = 100 X [(Test $^{51}$Cr released – Control $^{51}$Cr released) / (Maximum $^{51}$Cr released – Control $^{51}$Cr released)].

## G. Complement Dependent Cytotoxicity (CDC)

*Preparation of Target Cells*

Target cells were prepared by labeling NALM-6 or Daudi cells with $^{51}Cr$ and incubating them with antibody, as described for ADCC.

*$^{51}$Chromium Release Assay*

The amount of tumor cell lysis by complement proteins in the presence of antibody was determined using a $^{51}Cr$ release assay. This assay was identical to the one used for determining ADCC above with the exception of substituting effector cells with human or mouse serum. The labeled and antibody bound target cells were mixed with different dilutions of normal human serum (Valley Biomedical, Winchester, VA) in complete medium. Complete medium containing 2% Triton X-100 was used as a positive control to determine maximum $^{51}Cr$ release. Cells were then incubated for 4-18 hr in 5% $CO_2$ at 37°C. The plates were centrifuged, and the amount of radioactivity in the cell supernatants was determined using a gamma counter. Specific lysis was calculated using the same formula as used for ADCC.

**H. Pharmacokinetic (*Pk*) Analysis**

Female 6 to 8 weeks of age Swiss Webster mice were used to determine the *Pk* properties of the MAbs. Lugol's solution (Sigma, St Louis, MO) was added to their drinking water to a final concentration of 0.05% one day before injection and throughout the entire period of the experiment (168 h). Five mice were injected in the tail vein with 3 – 5 X $10^7$ cpm/100 µL radiolabeled MAbs, and whole body radioactivity was measured after injection and every 24 hr for 1 week in an AtomLab 100 dose calibrator (Atomic Product Corp., New York, NY). The radioactivity measured at different time points was expressed as the percentage of the initial radioactivity. The pharmacokinetic parameters, the beta phase of its half life ($T_{1/2}$), area under the curve (AUC), fractional catabolic rate (FCR), and mean residence time (MRT) were determined using a noncompartmental model with the PKCALC program[105] using data collected between 24 and 168 hr. $T_{1/2}$ indicates the amount time when half the amount of MAb is left in the body. The AUC indicates the bioavailability of MAb, or the amount absorbed in the blood. The MRT indicates how long the MAb stays in the blood, and the FCR indicates the amount of MAb catabolized or eliminated per day.

## I. Xenograft Tumor Models and Therapy

Two *in vivo* models were used. In the first model, the anti-tumor activities of the chimeric MAbs were compared to the murine MAb in SCID mice with $CD19^{lo}$ human pre-B ALL tumor xenografts. In the second model, SCID mice with $CD19^{hi}$ human Burkitt's lymphoma tumor xenografts were used to determine whether the difference in the valency of the chimeric MAbs could give better responses at lower doses.

### *SCID Mice*

For the xenograft experiments, female inbred CB.17 SCID mice were purchased from Taconic Farms (Taconic, Germantown, NY). All mice were housed in sterilized cages with filter tops in accordance with institutional animal care policy. Mice were allowed to acclimate in the facility for a minimum of seven days prior to handling. All protocols were approved by the University of Texas Southwestern Medical Center at Dallas institutional protocol review committee. The mice were 6-10 weeks of age at the time of tumor cell inoculation, as described below. Following tumor cell inoculation the mice were monitored for tumor development as determined by hind leg paralysis, as well as any signs of ill health as

determined by a loss of > 20% of their initial body weight.

*Pre-B Acute Lymphoblastic Leukemia Model (NALM-6 cells)*

SCID mice were weighed before tumor inoculation to establish a baseline weight. The mice were injected intravenously (i.v.) in the lateral tail vein with 5 X $10^6$ NALM-6 cells in 0.1 mL PBS 24 hr before treatment with MAbs. Groups of 5 mice were inoculated intraperitonealy (i.p.) with 7.5 µg/g or 10 µg/g body weight of divalent or tetravalent MAb, respectively, in four equal injections on days 1 to 4 after tumor inoculation. Mice were weighed and checked daily and were sacrificed at the onset of hind leg paralysis, a clinical symptom that accurately predicts death. Hind leg paralysis occurs due to the migration of the tumor cells into the spinal cord of the mice, thus paralyzing their hind legs. The mean paralysis time (MPT) was taken as the end point in this animal model.

*Burkitt's Lymphoma Model (Daudi cells)*

To determine the difference in the dose response of mice treated with divalent *versus* tetravalent chimeric MAb, SCID mice were inoculated intravenously with 5 X $10^6$ Daudi cells in 0.1 mL PBS 24 hr

before treatment with MAbs. Groups of 5 mice were inoculated i.p. with 7.5, 3.75 or 1.875 µg/g body weight cHD37 or 10, 5 or 2.5 µg/g body weight of cHD37-DcVV in four equal injections on days 1 to 4 after tumor inoculation. Mice were weighed and checked daily and were sacrificed at the onset of paralysis. The MPT was taken as the end point in this animal model.

**J. Statistical analysis**

Values for *in vitro* experiments were analyzed using a one-tail t test comparing MAb-treated samples with isotype control-treated samples, unless otherwise noted. Samples were considered to be significantly different when $p < 0.05$. For *in vivo* therapy data, MPT curves were compared using the Wilcoxon matched-pairs log-rank test. MPT curves were considered to be significantly different when $p < 0.05$.

# CHAPTER THREE

## Results

### A. Construction and Expression of the Chimeric MAbs

Two recombinant chimeric HD37 MAbs were constructed, one divalent and one tetravalent. HD37 was first chimerized to decrease its immunogenicity in humans. Because HD37 homodimers (i.e. two covalently conjugated IgG molecules) were previously found to be more effective than monomers at inducing cell death in tumor cells[98], the tetravalent antibody was constructed to create an antibody with the same valency as the homodimer. However, the advantages of the tetravalent *versus* homodimeric MAbs are that the tetravalent MAb is smaller in size, it retains normal Fc effector functions, and its activity should not be compromised by the conjugation chemistry. The structures of the MAbs are depicted in **Figure 1**. Like HD37, cHD37 has two murine variable regions composed of VL and VH regions, while cHD37-DcVV has four murine variable regions composed of two VLs and two VHs each joined together by the linker peptide SGGGGS. The constant regions of the recombinant MAbs are of human origin and are composed of human constant kappa chain (CL), and the CH1, CH2 and CH3 regions of human

IgG1. By retaining the variable regions of the murine HD37 antibody, the specificity of the recombinant MAbs is preserved.

The divalent cHD37 MAb was constructed by cloning the HD37 VH and VL genes into the human IgG1κ heavy and light chain expression vectors, pAH4604 and pAG4622 (**Figure 2**), respectively. The plasmids were co-transfected and expressed in SP2/0 cells. The tetravalent cHD37-DcVV MAb was constructed by cloning two pairs of the HD37 VH and VL genes into the pIZ-DcVV vector, and the plasmid was transfected and expressed in CHO cells. Stable transfectants were selected, and the yield of the highest cHD37 producer clone was 2-5 mg/L while the yield of cHD37-DcVV was greater than 22 mg/L. Both chimeric MAbs were purified to homogeneity by precipitation with ammonium sulfate followed by affinity chromatography on Protein G-Sepharose. The purity and molecular weight were assessed by SDS-PAGE (**Figure 3**). Under reducing conditions, murine HD37 and cHD37 yielded two protein bands with molecular masses of ~50 kDa (heavy chain) and ~25 kDa (light chain), whereas cHD37-DcVV yielded bands of ~70 kDa (heavy chain) and ~35 kDa (light chain). SDS-PAGE analysis under nonreducing conditions showed a single band of ~150 kDa for murine HD37 and cHD37 and a band of ~200 kDa for cHD37-DcVV. There were no

differences in the purity of the two constructs, and HPLC analysis showed that there were no aggregates or fragments in the preparations (**Figure 4**).

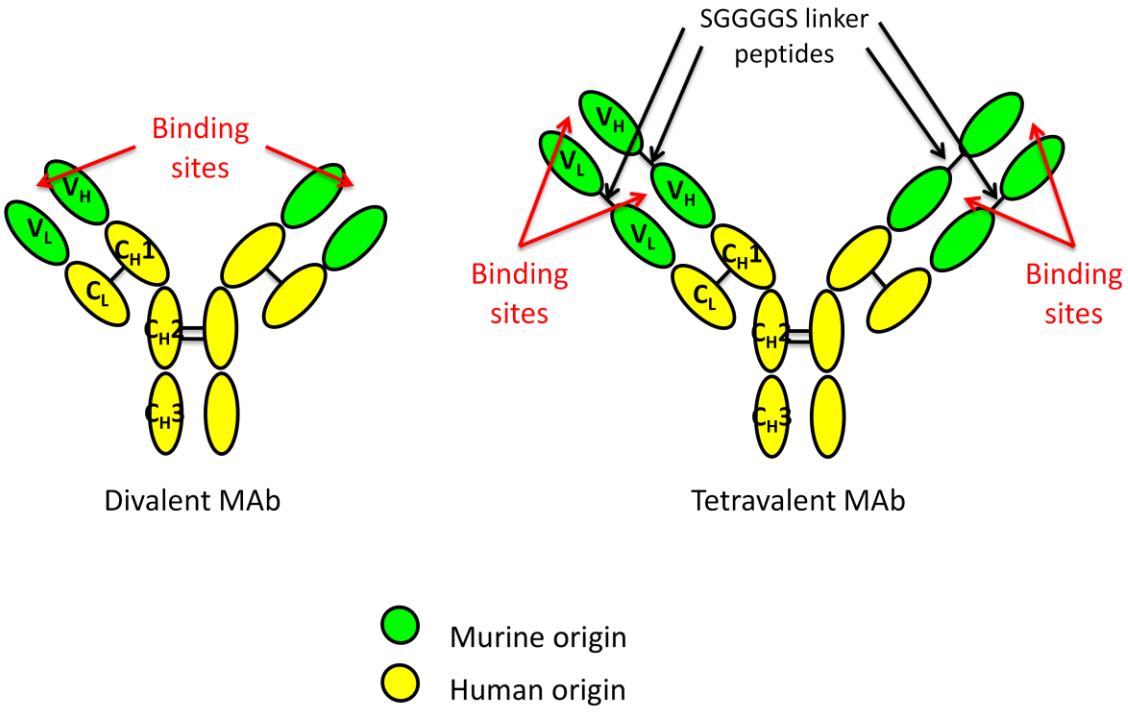


**Figure 1: Structure of the chimeric HD37 MAbs.**

The structures of the chimeric MAbs are depicted in a two-dimensional diagram. The divalent HD37 MAb has two binding sites while the tetravalent MAb has four. The antibodies are composed of murine HD37 variable domains (green) and human IgG1κ constant domains (yellow). The tetravalent antibody has four variable domains that are joined together in pairs by the short peptide linker, Ser-Gly-Gly-Gly-Gly-Ser.

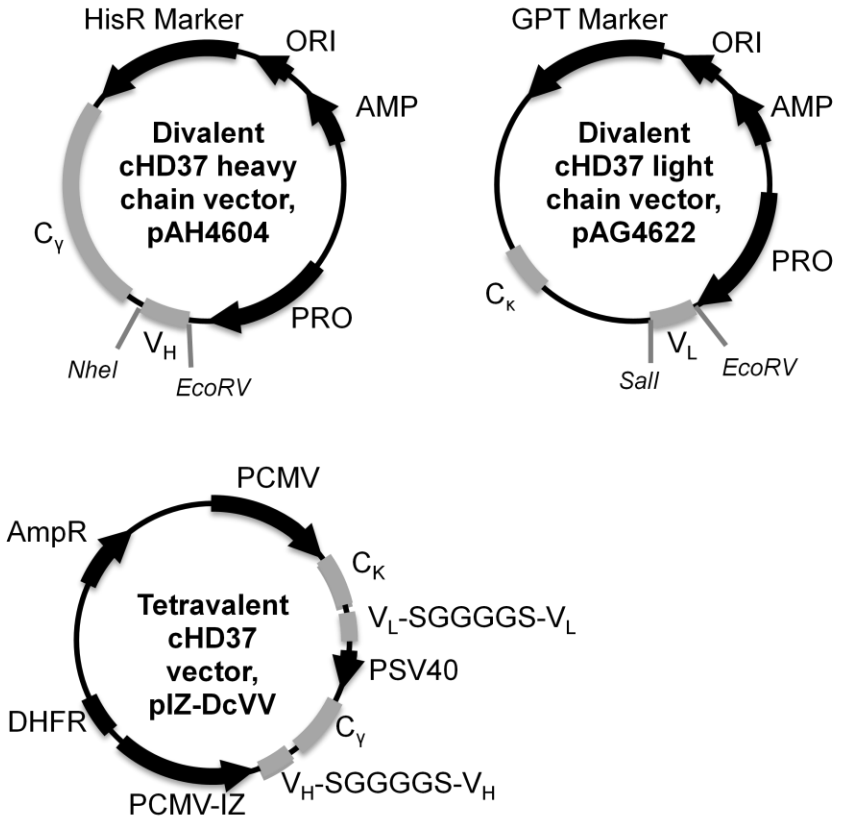


**Figure 2: Vectors for the construction of the chimeric HD37 MAbs.**

The divalent cHD37 MAb was constructed by cloning the HD37 VH and VL genes into the human IgG1κ heavy and light chain expression vectors, pAH4604 and pAG4622, respectively, while the tetravalent cHD37-DcVV MAb was constructed by cloning two pairs of the HD37 VH and VL genes into the pIZ-DcVV vector. AMP designates the β-lactamase gene; ORI, the origin of replication; PRO, the promoter; GPT Marker, the guanine phosphoribosyltransferase gene; HisR Marker, the histidinol resistance gene; PCMV-IZ, the cytomegalovirus promoter including cDNA encoding an intronic zeocin resistance gene that is expressed by alternative splicing; DHFR, the dihydrofolate reductase gene expression cassette; PCMV, the cytomegalovirus promoter; AmpR, the ampicillin resistance gene; and PSV40, the simian virus 40 promoter.

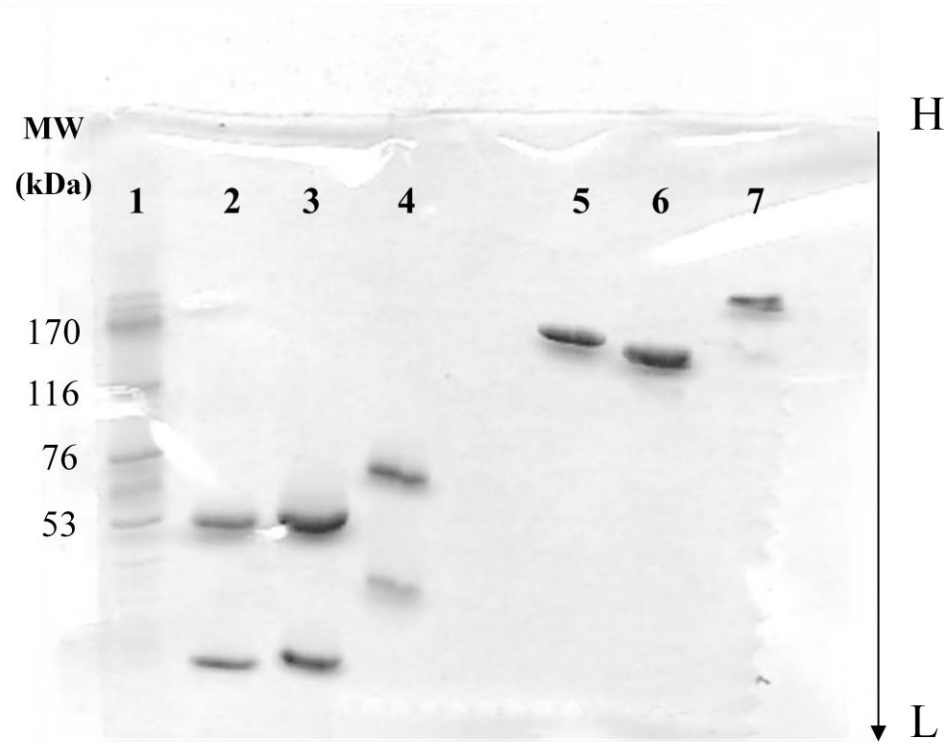


**Figure 3: SDS-PAGE analysis.**

Following the expression and purification of the chimeric HD37 MAbs, the MAbs were analyzed in a 4-15% gradient gel run under reduced (lanes 2–4) and unreduced (lanes 5–7) conditions to determine their molecular weights and purity. Lane 1, molecular weight markers; lanes 2 and 5, murine HD37; lanes 3 and 6, cHD37; lanes 4 and 7 cHD37-DcVV. This is one representative gel of three.

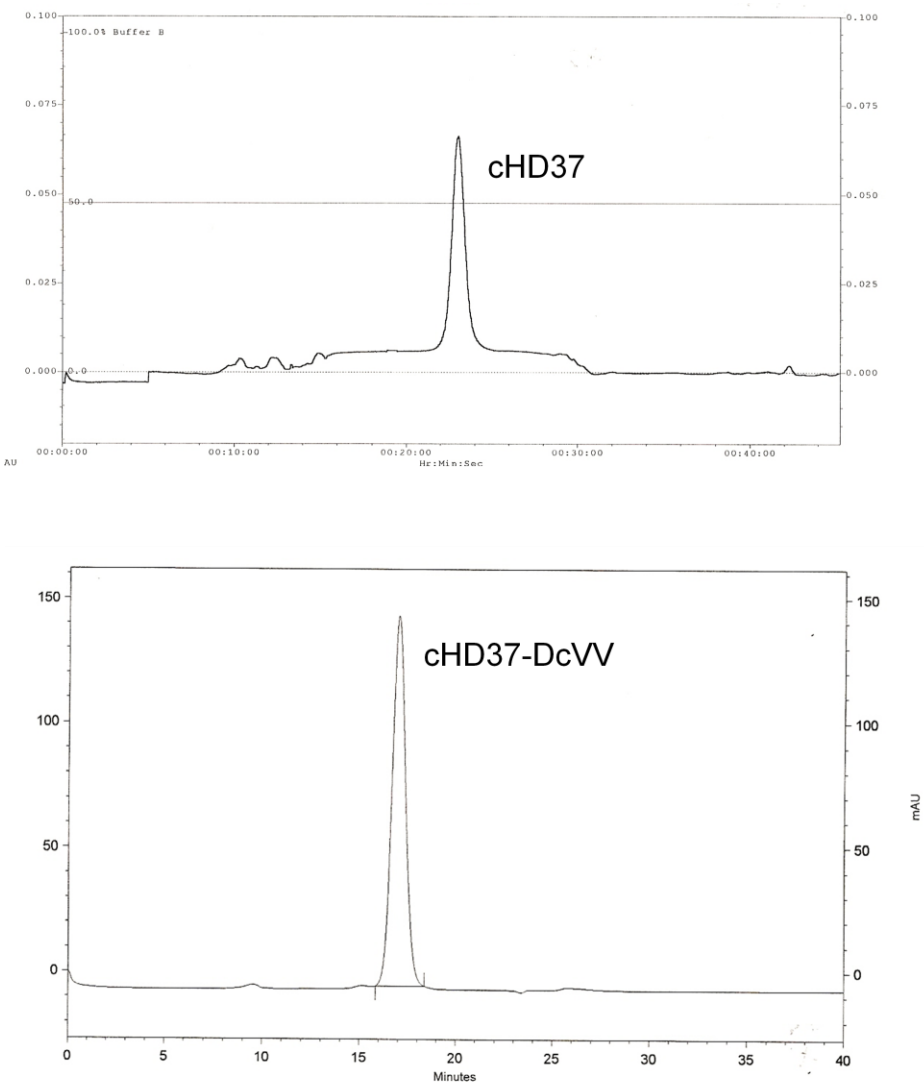


**Figure 4: HPLC analysis.**

HPLC analysis showed that there was no aggregation or fragmentation in the chimeric HD37 MAbs. The MAb preparation samples in PBS buffer, pH 7.4, were ran on a mobile phase HPLC with a single column (7.5mm diameter x 60cm length) at a flow rate of 1 mL/min at room temperature, and the samples were measured at 280 nm. This is one representative HPLC analysis of three for each MAb.

**B. Association and Dissociation of the MAbs to NALM-6 and Daudi Cells**

The results of SDS-PAGE analysis suggest that the structure of cHD37 is the same as HD37 while cHD37-DcVV contains two extra variable regions. The next series of experiments were designed to determine whether the recombinant MAbs were functionally similar to the murine MAb. First, FACS analysis was used to determine whether the recombinant MAbs bind to human $CD19^{+}$ pre-B ALL NALM-6 and Burkitt's lymphoma Daudi cells *in vitro*. NALM-6 and Daudi cells express low and high densities of CD19, respectively[86, 87]. cHD37 and cHD37-DcVV bound to both cells lines comparably regardless of the density of CD19 antigen on the cell surface (**Figure 5**). The FACS analyses indicate that the variable domains of the chimeric constructs are functionally the same as those of the parent antibody. The discrepancy seen in the binding of the murine *versus* chimeric MAbs may be due to the differences in the preparation of the MAbs (the murine MAb was prepared years prior and frozen in -140°F storage while the chimeric MAbs were freshly prepared weeks prior to the experiment), or in the secondary detection antibody used (goat anti-murine *versus* goat anti-human MAbs conjugated to FITC).

None of the HD37 MAbs were able to bind CD19$^-$ Jurkat cells (data not shown).

The relative binding affinities of cHD37-DcVV, cHD37 and the murine HD37 were compared using Scatchard analysis (**Figure 6**). The binding affinity of cHD37-DcVV was significantly higher ($p < 0.05$) than that of the murine HD37 for both NALM-6 and Daudi cells (**Figure 7**). Furthermore, the binding affinity of cHD37-DcVV was significantly higher than that of cHD37 for Daudi cells, which indicates that the tetravalent MAb has a higher relative binding affinity than either of the divalent MAbs. These results suggest that more than two binding sites of the tetravalent MAb are able to bind simultaneously.

The dissociation of the radiolabeled tetravalent *vs.* divalent MAbs from NALM-6 and Daudi cells in the presence of the same cold competitor (HD37) was compared, and the persistence of the MAbs on the cell surface was calculated from the dissociation curves (**Figure 8**) and expressed as a half-life ($T_{1/2}$) of dissociation. The $T_{1/2}$ of dissociation of cHD37-DcVV was significantly longer than that of the murine HD37 and cHD37 for both cell lines (**Figure 9**). The results demonstrate that the strength of binding depends on the valency of the constructs.

In summary, the results of these experiments suggest that the tetravalent MAb has more than two functional binding sites, and more than

two sites bind antigen simultaneously. This contributes to the increased relative binding affinity of the tetravalent MAb. In addition, the increased multivalency of the tetravalent MAb results in a slower off rate from cells.

**(A)**

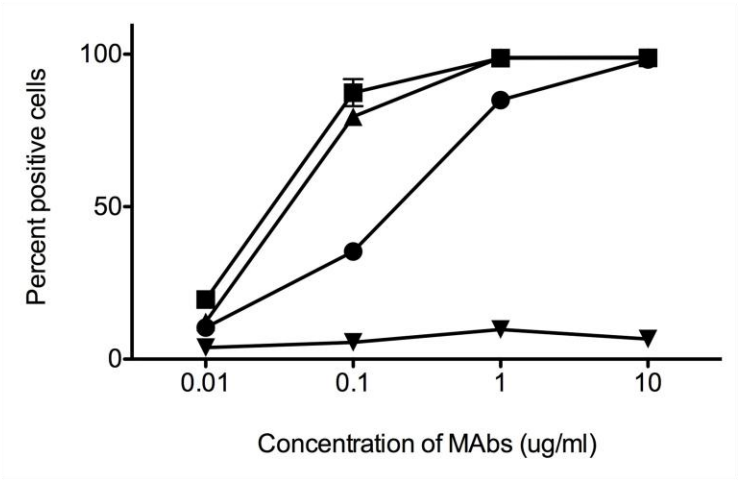


**(B)**

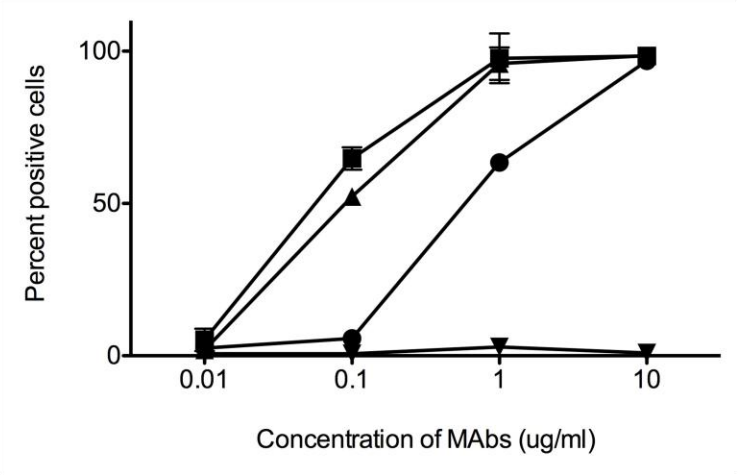


**Figure 5: Binding of HD37 MAbs to pre-B ALL NALM-6 and Burkitt's lymphoma Daudi cells (FACS analysis).**

The ability of the MAbs to bind $CD19^+$ (A) NALM-6 and (B) Daudi cells was assessed by flow cytometry. Circles, HD37; squares, cHD37; triangles, cHD37-DcVV; and inverted triangles, isotype control MOPC-21. Data represent means ± SD of three experiments for each cell type.

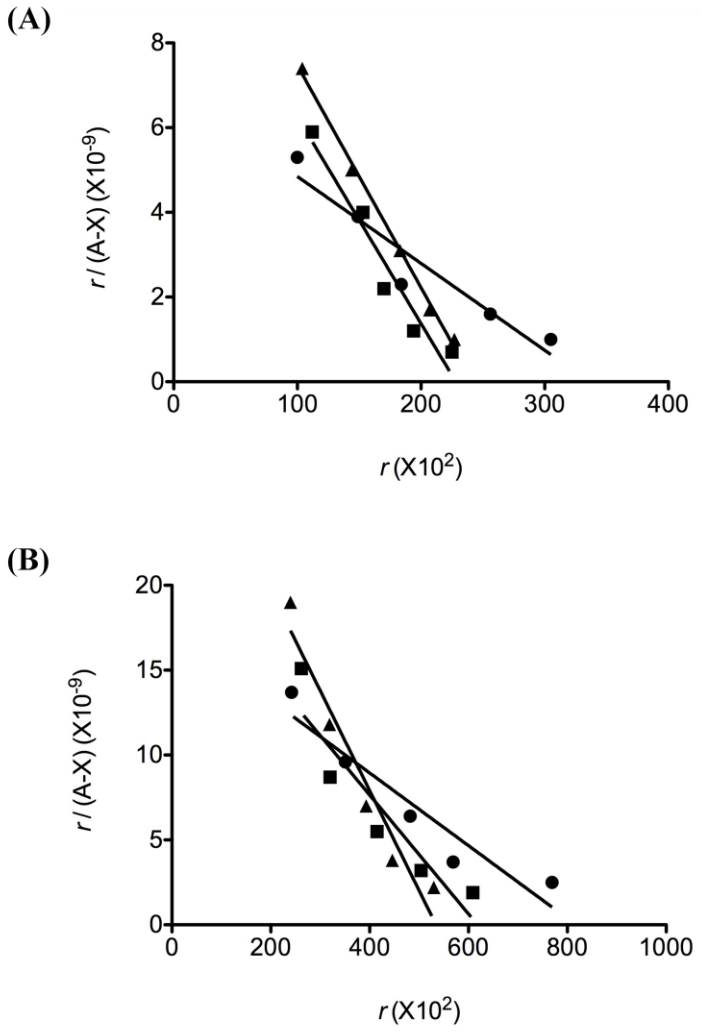


**Figure 6: Affinity of the HD37 MAbs for NALM-6 and Daudi cells (Scatchard plot).**

The ability of the MAbs to bind $CD19^+$ (A) NALM-6 and (B) Daudi cells was also assessed by Scatchard analysis. Circles, HD37; squares, cHD37; and triangles, cHD37-DcVV. This is one representative experiment of three performed for each cell type. Abbreviations: A = the initial concentration of the antibody; A–X = the concentration of the unbound antibody; X = the concentration of the immune complex; r = the number of antibody molecules bound per cell.

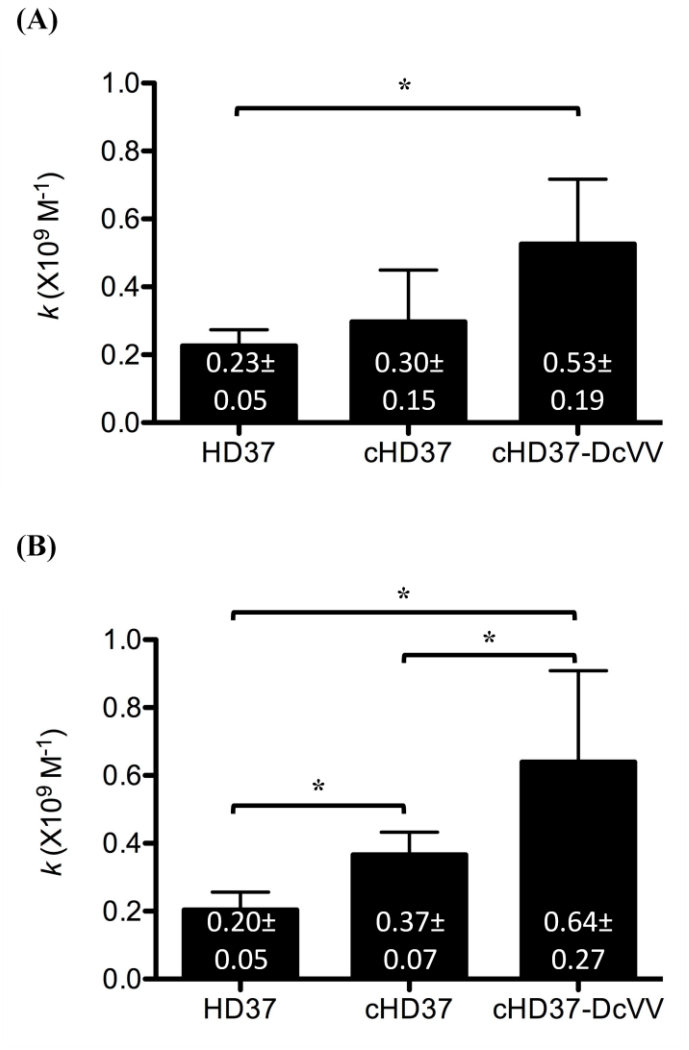


**Figure 7: Binding affinity (*k*) of the HD37 MAbs.**

The binding affinity (*k*) of the MAbs to (A) NALM-6 and (B) Daudi cells was determined by Scatchard analysis. The *k* values are shown in the bars. The *k* values of HD37 *vs.* cHD37-DcVV are significantly different ($p < 0.05$) for NALM-6 cells. The *k* values of HD37 *vs.* cHD37, HD37 *vs.* cHD37-DcVV, and cHD37 *vs.* cHD37-DcVV are significantly different for Daudi cells. Data represent means ± SD of three experiments for each cell type. * = signficant

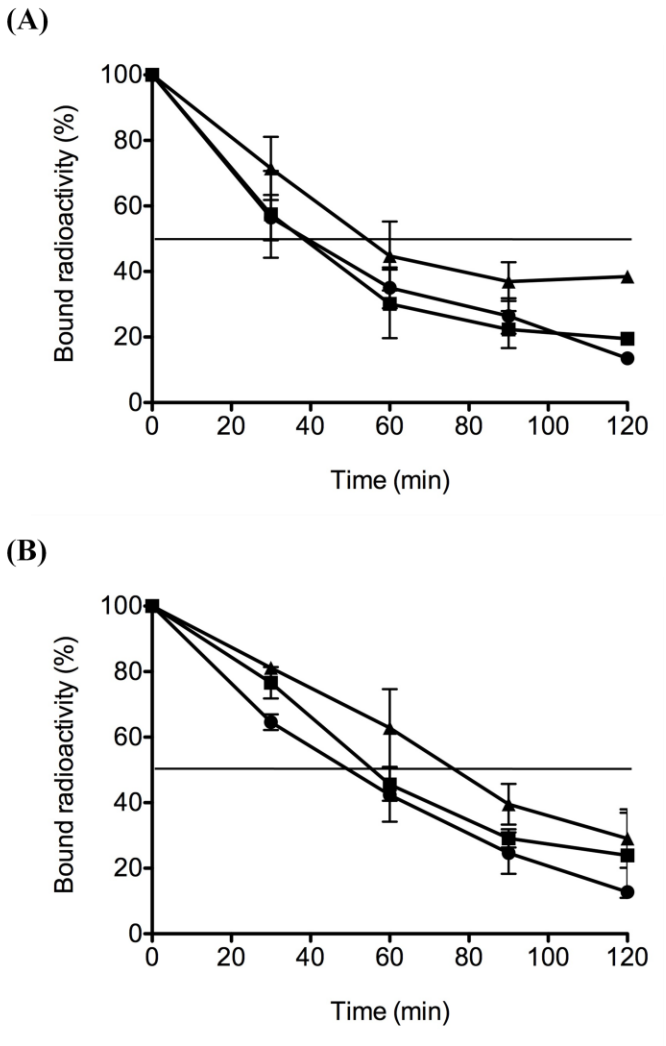


**Figure 8: Dissociation of the HD37 MAbs from NALM-6 and Daudi cells.**

The persistence of the MAbs on the cell surface of (A) NALM-6 and (B) Daudi cells was calculated from the dissociation curves and expressed as a half-life ($T_{1/2}$) of dissociation. Circles, HD37; squares, cHD37; and triangles, cHD37-DcVV. Data represent means ± SD of three experiments for each cell type.

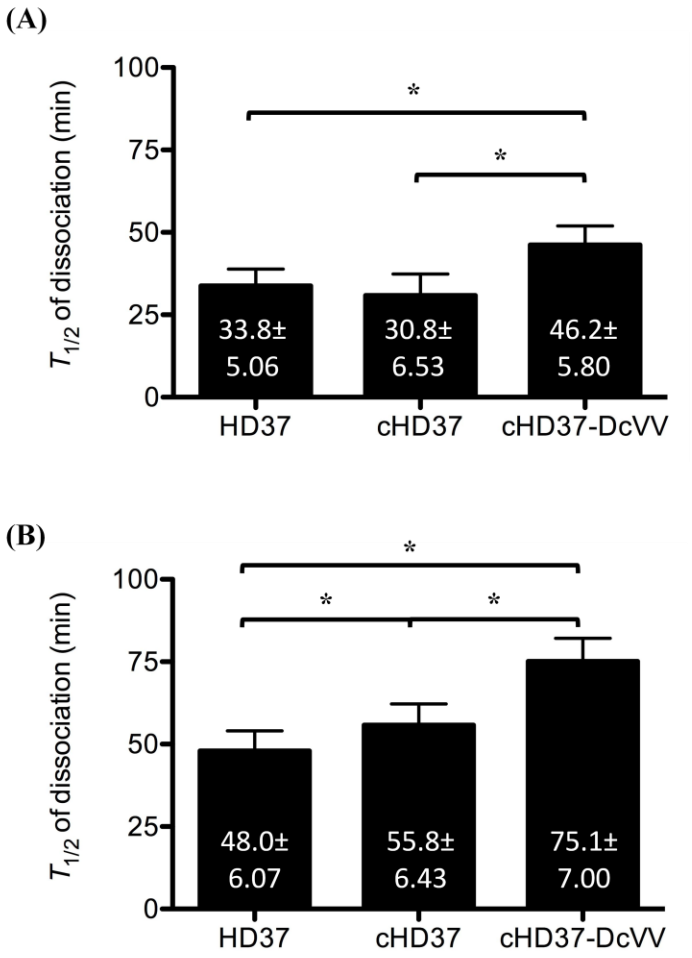


**Figure 9: $T_{1/2}$ of dissociation of the HD37 MAbs.**

The $T_{1/2}$ of dissociation of the MAbs from (A) NALM-6 and (B) Daudi cells was determined by dissociation analysis. The values are shown in the bars. The $T_{1/2}$ of dissociation HD37 *vs.* cHD37-DcVV and cHD37 *vs.* cHD37-DcVV are significantly different ($p < 0.05$) for NALM-6 cells. The $T_{1/2}$ of dissociation of HD37 *vs.* cHD37, HD37 *vs.* cHD37-DcVV, and cHD37 *vs.* cHD37-DcVV are significantly different ($p < 0.05$) for Daudi cells. Data represent means ± SD of least three experiments performed for each cell type. * = significant

**C. Binding of the MAbs to U937 Cells**

The next set of experiments was designed to assess the effector functions of the Fc regions of the different HD37 MAbs. As previously mentioned, chimerizing HD37 can optimize its effector functions and *Pk* properties in humans. The effector functions are affected because the Fc region of a human MAb will bind FcRs on human effector cells more efficiently than would the Fc region of a mouse MAb, such as human IgG1 binding human FcγRI and FcγRIII[106]. Although both murine and human IgG1 bind murine FcγRI[106, 107] and FcγRIII[108-112] comparably well, murine IgG1 binds poorly to human FcγRI[113-117] and FcγRIII[118, 119].

FACS analysis was used to evaluate the relative binding affinities of the MAbs to human FcγRI$^{+}$FcγRIII$^{+}$CD19$^{-}$ U937 cells, a human leukemic monocytic lymphoma cell line. The binding of a MAb to both FcγRs is dependent upon the presence of an intact Fc region. There was no significant difference in the binding of cHD37 compared to that of cHD37-DcVV (**Figure 10**). As expected, the murine HD37 bound poorly to human U937 cells. These results clearly indicate that the chimeric HD37 MAbs have functional and intact Fc regions, and therefore, they should interact with human FcγRI and III-bearing effector cells and mediate effector functions.

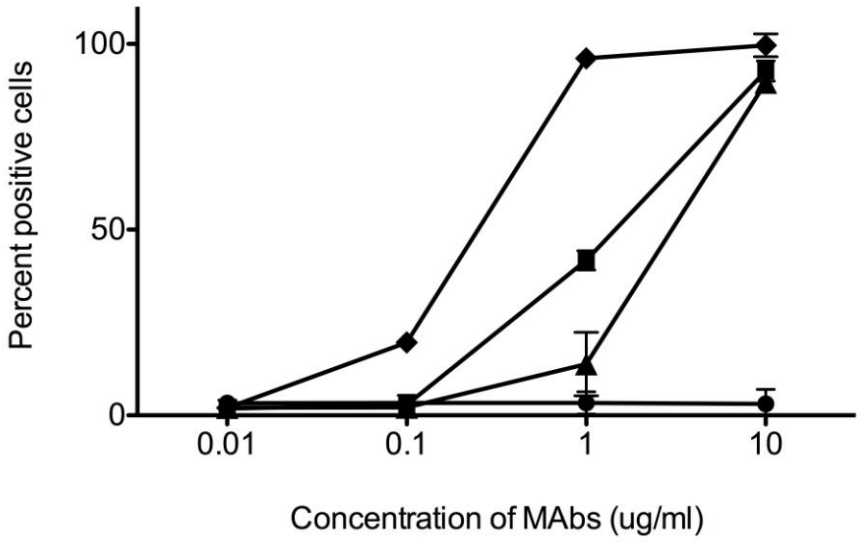


**Figure 10: Binding of HD37 MAbs to U937 cells (FACS analysis).**

The ability of the MAbs to bind human FcγRI$^{+}$FcγRIII$^{+}$CD19$^{-}$ U937 cells was assessed by flow cytometry. Circles, HD37; squares, cHD37; triangles, cHD37-DcVV; and diamonds, positive control chimeric cUV3 MAb. Data represent means ± SD of three experiments.

**D. ADCC and CDC Activity of the MAbs**

Since the chimeric MAbs were able to bind to cells expressing human FcγRI and FcγRIII, the next set of experiments was designed to test the ability of the HD37 MAbs to mediate ADCC against NALM-6 or Daudi target cells using human NK or murine LAK effector cells. The activity of the tetravalent MAb was compared to that of the divalent MAbs. As expected, murine HD37 did not mediate ADCC when human NK cells were used due to the inability of the murine Fc to bind human FcRs **(Figure 11**). In contrast, when human NK effector cells were used, the chimeric MAbs mediated ADCC against the target cells. Moreover, cHD37-DcVV was more effective at lysing the target cells than cHD37 and the difference was more pronounced over time (**Figure 11 and 12**). However, when using murine LAK effector cells, ADCC against both NALM-6 and Daudi target cells of all three MAbs was comparable (**Figure 13**).

The abilities of the MAbs to mediate CDC against target cells were measured using either human or mouse sera as sources of complement. None of the MAbs were able to lyse NALM-6 target cells using human complement, while the cHD37-DcVV was the only MAb to mediate efficient CDC using human complement against Daudi cells (**Figure 14**).

Previous studies have also shown that human complement mediated lysis is highly variable among cell lines[49, 120], which correlates with our findings that CDC was effective against Daudi, but not NALM-6 cells. None of the MAbs were able to lyse target cells when mouse complement was used (data not shown).

These results demonstrate that the chimeric MAbs have functional Fc domains and further indicate that the *in vitro* efficacy of the MAbs depends on the type of cells or complement proteins that mediate effector functions.

Hence the tetravalent MAb was better than the divalent MAbs at mediating ADCC when using human effector cells, and equally effective as the divalent MAbs when using murine effector cells. The tetravalent MAb was also the only construct that could mediate CDC against Daudi cells when human complement was used. Therefore, in humans with human effector cells and complement, the tetravalent MAb may be more effective than the divalent MAbs.

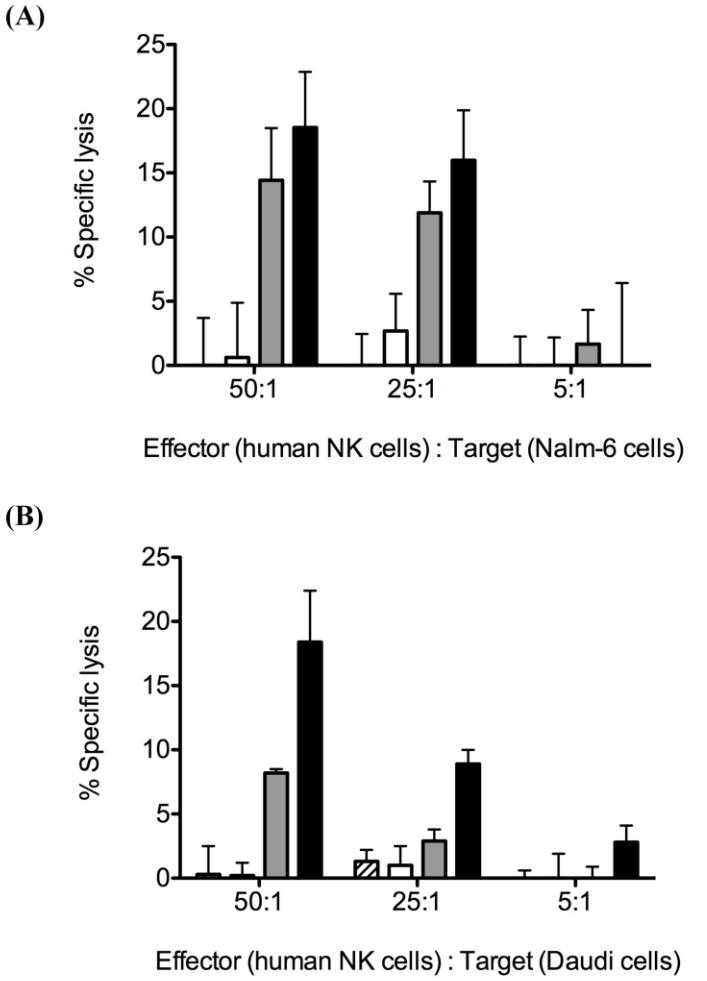


**Figure 11: ADCC with human NK effector cells.**

The ability of the HD37 MAbs to mediate ADCC against target (A) NALM-6 or (B) Daudi target cells using human NK effector cells. The background was subtracted to calculate the % specific lysis in each group. Diagonal bars, MOPC-21 (leftmost bar in each E:T ratio set and is not detectable except for standard deviations because the % specific lysis is near zero); white bars, HD37; gray bars, cHD37; and black bars, cHD37-DcVV. The % specific lysis of HD37 *vs.* cHD37, HD37 *vs.* cHD37-DcVV, and cHD37 *vs.* cHD37-DcVV are significantly different ($p < 0.05$) for E:T ratios at 50:1 and 25:1 for NALM-6 cells and at all three E:T ratios tested for Daudi cells. This is one representative experiment of three performed for each cell type.

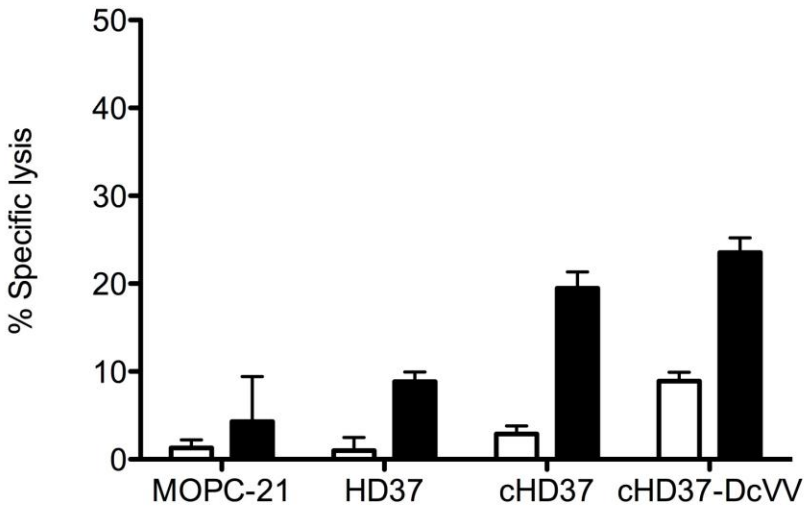


**Figure 12: Time dependent ADCC with human NK effector cells against target Daudi cells.**

The ability of the HD37 MAbs to mediate ADCC against Daudi target cells over time was evaluated. The E:T ratio was 25:1. Similar results were obtained at E:T ratios of 50:1 and 5:1. White bars, 6 hr lysis; and black bars, 18 hr lysis. Data expressing means ± SD are one representative experiment of three.

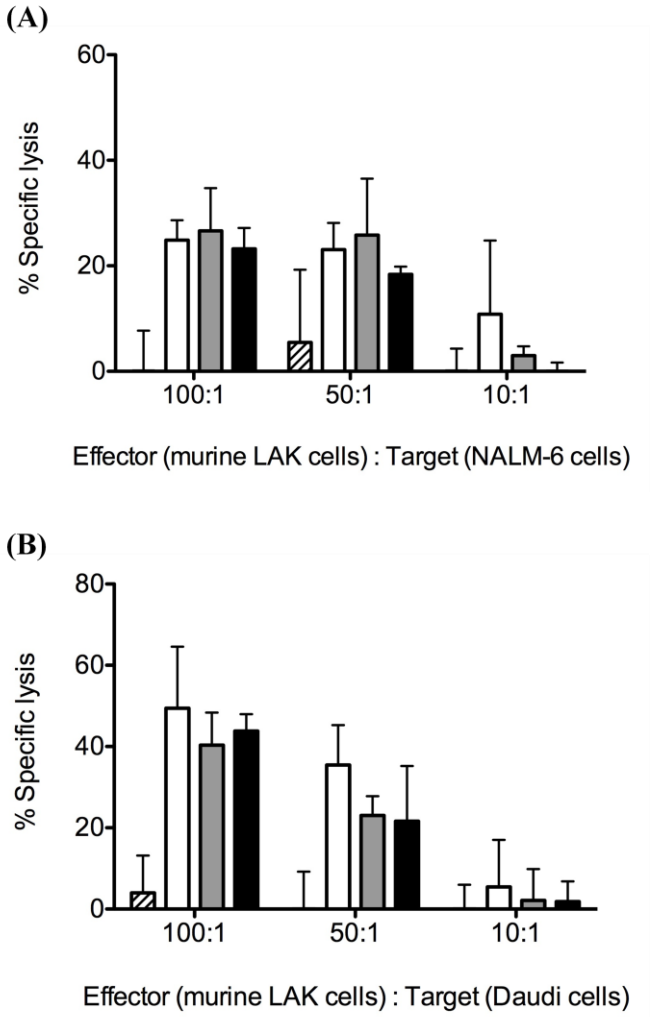


**Figure 13: ADCC with murine LAK effector cells.**

The ability of the HD37 MAbs to mediate ADCC against (A) NALM-6 or (B) Daudi target cells using murine LAK effector cells. The background was subtracted out to calculate the % specific lysis in each group. Diagonal bars, MOPC-21; white bars, HD37; gray bars, cHD37; and black bars, cHD37-DcVV. The % specific lysis of HD37 *vs.* cHD37 *vs.* cHD37-DcVV, are not significantly different ($p > 0.05$) at all E:T ratios for both NALM-6 and Daudi cells. This is one representative experiment of three performed for each cell type.

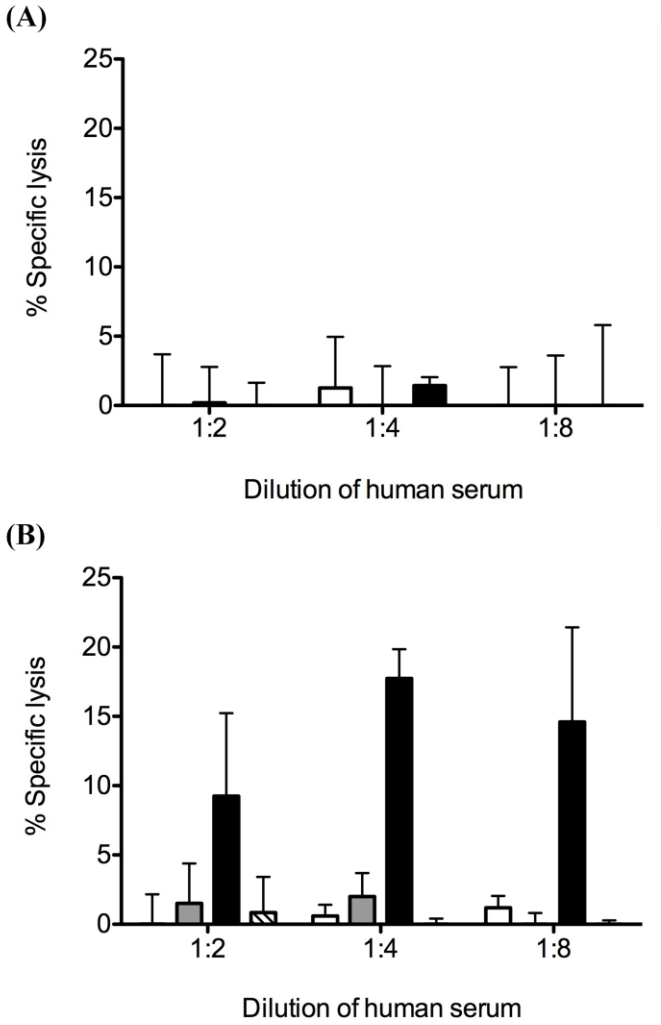


**Figure 14: CDC with human complement.**

The ability of the HD37 MAbs to mediate CDC against (A) NALM-6 or (B) Daudi target cells using human serum as a source of human complement proteins was evaluated. The background was subtracted out to calculate the % specific lysis in each group. Diagonal bars, MOPC-21; white bars, HD37; gray bars, cHD37; and black bars, cHD37-DcVV. The % specific lysis of HD37 *vs.* cHD37-DcVV and cHD37 *vs.* cHD37-DcVV, are significantly different ($p < 0.05$) at all dilutions for Daudi cells. This is one representative experiment of three performed for each cell type.

**E. Inhibition of Cell Growth**

The inhibition of the growth of NALM-6 and Daudi cells by the various MAb constructs in the absence of effector cells or complement was determined by two proliferation assays, [$^3$H]thymidine incorporation and MTS. [$^3$H]thymidine incorporation assesses cell growth by measuring the amount of radionuclide incorporated into proliferating cells undergoing DNA synthesis[121]. In an MTS assay, cell viability is determined in a colorimetric method measuring the chemical reduction of a tetrazolium compound (MTS) by metabolically active cells[122]. The growth of NALM-6 or Daudi cells cultured in the presence of increasing concentrations of murine, chimeric divalent or chimeric tetravalent HD37 was followed for 72 hr. None of the constructs had any effect on cell viability and their proliferative capacity even at concentrations of $10^{-6}$ M (**Figure 15**). Therefore, the primary mechanisms of action of the MAbs are mediated by ADCC and CDC.

To ensure that there was no *in vitro* effects of the MAbs on normal human B cells, the inhibition of the growth of LPS-activated normal human B cells by the MAb in the absence of effector cells or complement was also determined. None of the constructs had any effect on cell viability or proliferation (**Figure 16**).

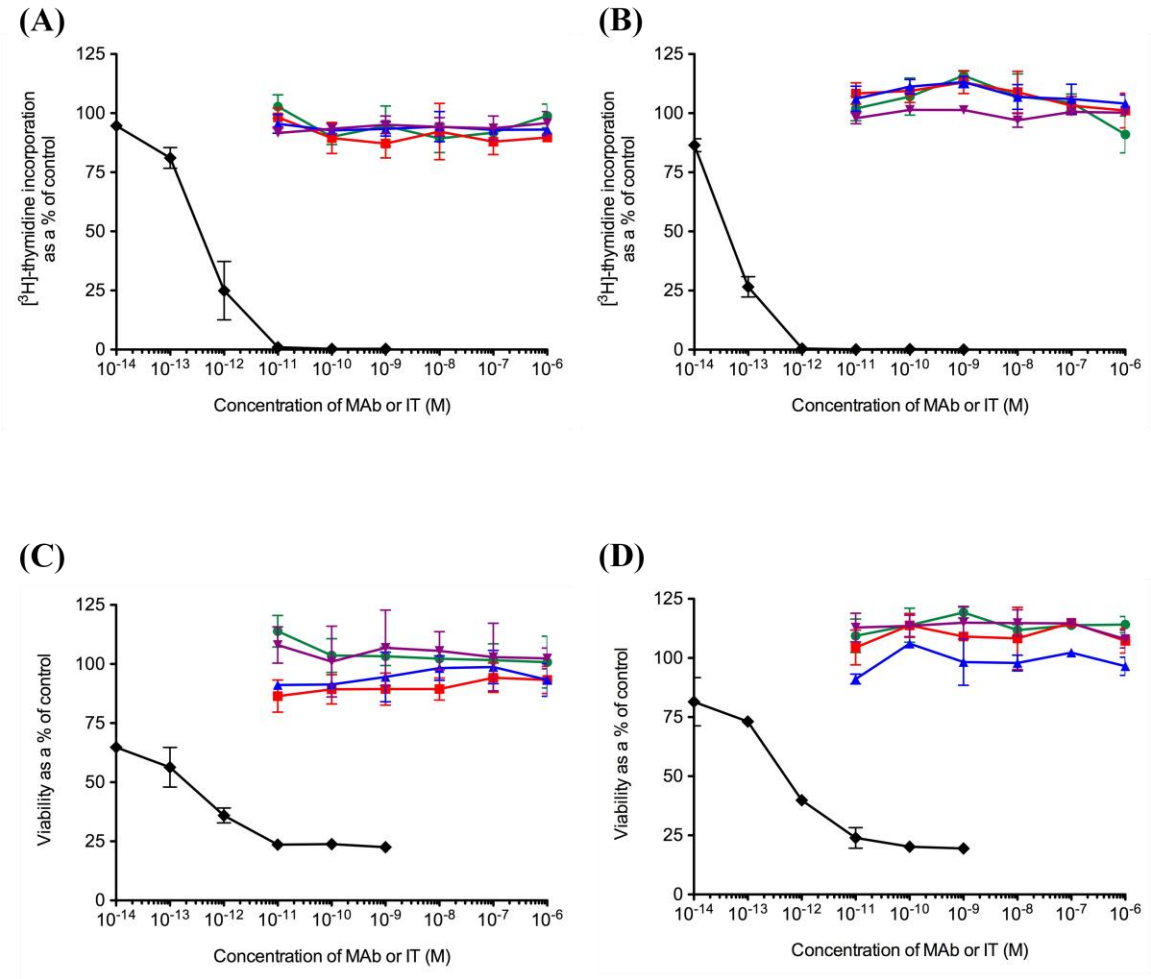


**Figure 15: Inhibition of tumor cell growth in the absence of effector cells and complement.**

The cytotoxic effects of the HD37 MAbs on (A and C) NALM-6 and (B and D) Daudi cells were evaluated by (A and B) [$^3$H]thymidine incorporation and (C and D) MTS assays. Green circles, HD37; red squares, cHD37; blue triangles, cHD37-DcVV; purple inverted triangles, MOPC-21; black diamonds, positive control HD37-dgA immunotoxin. Data represent means ± SD of three experiments for each type of cell and assay.

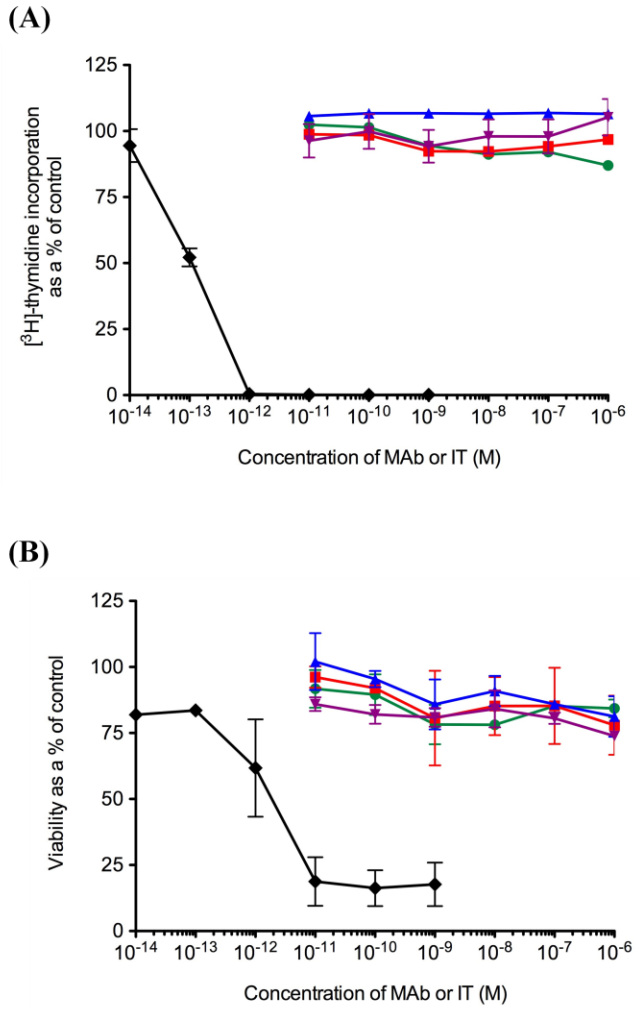


**Figure 16: Inhibition of LPS-activated normal human B cell growth in the absence of effector cells and complement.**

The cytotoxic effects of the HD37 MAbs on LPS-activated normal human B cells were evaluated by (A) [$^3$H]thymidine incorporation and (B) MTS assays. Green circles, HD37; red squares, cHD37; blue triangles, cHD37-DcVV; purple inverted triangles, MOPC-21; black diamonds, positive control HD37-dgA immunotoxin. Data represent means ± SD of three experiments for each type of assay.

**F. Pharmacokinetics**

The *Pk*s of the HD37 constructs were measured to determine whether the chimeric HD37 MAbs retained the *Pk* properties as murine HD37 *in vivo*. The *Pk*s were measured in Swiss Webster mice. This is a valid comparison since human and murine IgG have relatively similar affinities for murine FcRn ($R_{eq}$ of hIgG1-mFcRn *versus* mIgG1-mFcRn are 243.8 *versus* 100.6, respectively, a 2.4 fold difference) as compared to the affinities of human and murine IgG to human FcRn ($R_{eq}$ of hIgG1-hFcRn *versus* mIgG1-hFcRn are 91.8 *versus* 0.22, respectively, a 417 fold difference)[123]. Therefore human and murine IgG1 tend to have similar half-lives in mice[124]. As expected, the *Pk*s of the HD37 constructs were comparable in Swiss Webster mice based on the parameters measured (**Table 1**). The $T_{1/2}$ of the murine HD37 (302 hr), cHD37 (353 hr), and cHD37-DcVV (311 hr) were not significantly different ($p < 0.05$).

| MAb | $T_{1/2}$ (hr) | AUC | FCR ($day^{-1}$) | MRT (hr) |
|---|---|---|---|---|
| Murine HD37 | 302.2 ± 32.4 | 40131 ± 5932 | 0.055 ± 0.007 | 436.5 ± 46.8 |
| cHD37 | 352.5 ± 49.6 | 44253 ± 6288 | 0.047 ± 0.007 | 506.8 ± 71.6 |
| cHD37-DcVV | 311.1 ± 30.2 | 40557 ± 4722 | 0.053 ± 0.006 | 447.7 ± 43.6 |

**Table 1: Pharmacokinetics of the HD37 MAbs in Swiss Webster mice.**

Groups of five mice were used for each antibody tested. Values represent means ± SD of three experiments. $T_{1/2}$ = half life (beta phase); AUC = area under the curve; FCR = fractional catabolic rate; MRT = mean residence time.

**G. Therapeutic Efficacy of the HD37 Constructs in SCID Mice with Human Tumor Cell Line Xenografts**

Two cells lines, the pre-B ALL NALM-6 cell line and the Burkitt's lymphoma Daudi cell line, were used to test the therapeutic efficacy of the HD37 constructs *in vivo* in SCID mice with human cell line xenografts. The $CD19^{lo}$ NALM-6 cell line was used to determine whether the constructs would extend the mean survival time of SCID mice with pre-B ALL tumors and to compare their anti-tumor efficacy. In addition, similar experiments were carried out with Daudi cells to determine whether there was a correlation between the valency of the chimeric MAbs and the therapeutic dose required for optimal anti-tumor effects.

**NALM-6.** The therapeutic effects of the HD37 Mabs were evaluated in SCID mice injected with $5 \times 10^6$ NALM-6 tumor cells. The Kaplan-Meier survival curves were plotted and compared using the log-rank test. As previously described, groups of 5 mice were injected with $5 \times 10^{-11}$ mol/g (7.5 µg/g for divalent MAbs and 10 µg/g for tetravalent MAb). The dose selected was based on previous studies comparing murine HD37 to Rituxan[87, 94]. All three MAbs significantly improved the MST of SCID mice bearing disseminated NALM-6 tumors as compared to PBS and the MOPC-21 isotype-matched IgG1 control **(Figure 17)**. However, there was

no difference in the survival of the groups treated with murine HD37 (66 days), cHD37 (75 days) or cHD37-DcVV (63 days) MAbs. This may be explained by the fact that the optimal anti-tumor activity is dependent upon the type of effector cells present, and since mice lack human effector cells, the constructs showed no differences. The results also suggest that an increase in valency per se might not result in better *in vivo* activity in mice in the absence of effector cells that bind to the Fc of the antibody.

**Daudi.** The correlation between the valency of the MAb and the therapeutic dose required for optimal anti-tumor activity was evaluated in SCID mice injected with 5 X $10^6$ Daudi tumor cells. The Kaplan-Meier survival curves were compared using the log-rank test. Groups of 5 mice were injected with 5, 2.5 or 1.25 X $10^{-11}$ mol/g body weight cHD37 (7.5, 3.8, or 1.9 μg/g) or cHD37-DcVV (10, 5, or 2.5 μg/g). Although all treatment regimens significantly extended the MST of SCID/Daudi mice compared to the PBS control, there was no difference in the survival of mice treated with either the chimeric divalent or tetravalent MAbs at equivalent doses **(Figure 18)**. Therefore, this *in vivo* experiment further supports the finding that the activity of chimeric antibodies cannot be accurately compared in mice.

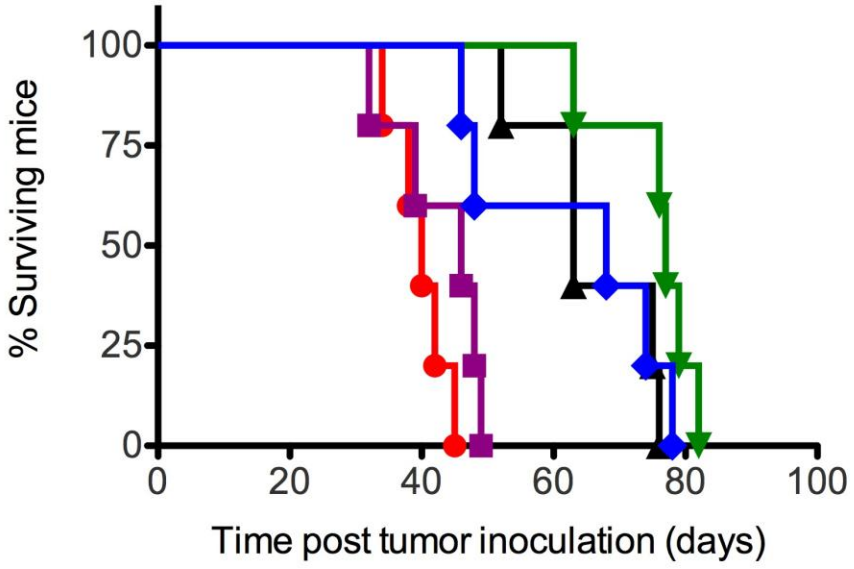


**Figure 17: Therapeutic efficacy of the HD37 constructs in SCID mice with NALM-6 tumor cell xenografts.**

The therapeutic efficacy of the HD37 MAbs in SCID mice with a disseminated $CD19^{lo}$ NALM-6 pre B cell tumor was evaluated. Female SCID mice, 6-8 weeks of age, were injected with 5 X $10^6$ NALM-6 tumor cells and treated on days 1 through 4 post-tumor inoculation with HD37 MAb constructs. Although each HD37 MAb treatment significantly extended the MST of SCID/NALM-6 mice ($p < 0.05$) as compared to PBS and MOPC-21 isotype-matched control, there was no significant difference in the survival between each HD37 MAb treatment group. Red circles, PBS; purple squares, 7.5 µg/g MOPC-21; black triangles, 7.5 µg/g HD37; green inverted triangles, 7.5 µg/g cHD37; and blue diamonds, 10 µg/g cHD37-DcVV. This figure depicts a single experiment with 5 mice per group and is representative of three separate experiments.

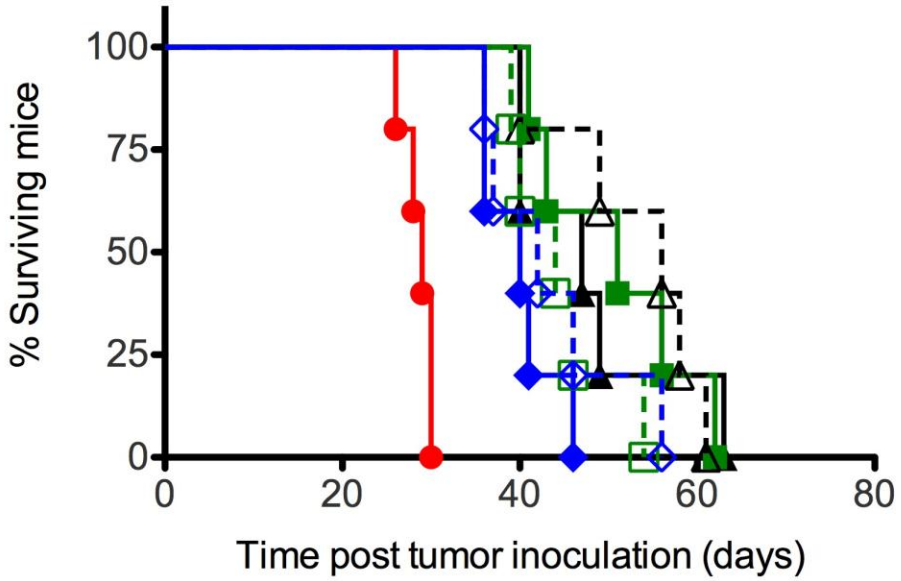


**Figure 18: Therapeutic efficacy of the HD37 constructs in SCID mice with Daudi tumor cell xenografts.**

The correlation between the valency of the MAb and the therapeutic dose required for optimal anti-tumor activity was evaluated in SCID/Daudi mice was evaluated. Female SCID mice, 6-8 weeks of age, were injected with 5 X $10^6$ Daudi tumor cells and treated on days 1 through 4 post-tumor inoculation with different doses of the chimeric HD37 MAbs. Although each chimeric HD37 MAb treatment significantly extended the MST of SCID/Daudi mice ($p < 0.05$) as compared to PBS and MOPC-21 isotype-matched control, there was no significant difference in the survival of mice treated with either the chimeric divalent or tetravalent MAbs at equivalent doses. Red circles, PBS; solid black triangles, 7.5 µg/g cHD37; solid green squares, 3.8 µg/g cHD37; solid blue diamonds, 1.9 µg/g cHD37; open black triangles, 10 µg/g cHD37-DcVV; open green squares, 5 µg/g cHD37-DcVV; open blue diamonds, and 2.5 µg/g cHD37-DcVV. This figure depicts a single experiment with 5 mice per group and is representative of three separate experiments.

# CHAPTER FOUR

## Discussion

### A. Study Objectives and Major Findings

Pre-B ALL affects thousands of children and adults in the United States every year[3]. Because the recommended treatment (chemotherapy and bone marrow transplantation) is highly myelosuppressive, cytotoxic to healthy tissues and invasive, targeted MAb therapy is emerging as an important treatment modality[17]. Currently, the only FDA approved MAbs for B cell malignancies are anti-CD20 based therapies[125]. However, pre-B ALLs do not express CD20[68]. CD19 is a 95 kDa glycoprotein exclusively expressed on B cells from the early stages of B cell development until just prior to their terminal differentiation into plasma cells[68, 126]. CD19 is expressed on many B cell malignancies including pre-B ALLs and B cell lymphomas[68]. CD19 is therefore an attractive target for immunotherapies against pre-B ALLs, B cell tumors that have lost CD20 expression, and alternative regimens for patients who are refractory to anti-CD20 treatment.

A mouse MAb against human CD19, HD37[87], has been studied extensively. Previous studies have shown that HD37 inhibits the growth of

human B cell tumor lines *in vitro* and extends the mean survival time of SCID mice with human B cell tumors[87]. Furthermore, when conjugated to dgRTA, HD37 has been used as an IT to treat patients with both B cell lymphomas and pre-B ALL[96, 97]. However, the long term clinical application of unconjugated HD37 is limited because mouse MAbs are highly immunogenic, have short serum half-lives, and their Fc portions are unable to mediate effector functions in humans[127].

Although most MAbs in cancer therapy function through the recruitment of secondary immune effector mechanisms[25], previous reports have also shown that that some MAbs can induce growth arrest and/or apoptosis of the tumor cells[19, 128, 129]. In the case of HD37, homodimers consisting of two chemically conjugated IgG molecules, but not IgG itself, induced cell death in tumor cells, presumably due to hypercrosslinking and/or a slower dissociation rate[98]. However, their large size prevents effective tumor penetration, and normal Fc effector functions are often not retained thereby limiting their therapeutic potential.

The objectives of this study were to construct, express, and test the *in vitro* and *in vivo* activities of divalent chimeric and tetravalent chimeric HD37 MAbs with the goal of using these data to determine which chimeric HD37 to move forward into clinical trials. Chimeric MAbs, which are MAbs with human constant regions and mouse variable regions, are far less

immunogenic than their mouse counterparts and can efficiently carry out effector functions in humans due to their ability to engage human effector cells and complement with their Fc regions. Tetravalent MAbs, which are MAbs with one human Fc and four mouse variable regions, are smaller in size than their homodimeric counterparts and can carry out normal effector functions. The activities of the two cHD37 MAbs (divalent and tetravalent) were compared to each other as well as to that of the murine HD37.

The major findings to emerge from this study are that 1) all three forms of HD37 were equally effective at extending the mean survival time of SCID mice with human pre-B ALL and Burkitt's lymphoma tumors; and 2) the tetravalent cHD37 was more effective than the murine HD37 and divalent cHD37 at mediating secondary effector functions *in vitro* with human effector cells and complement. These findings suggest that whereas the tetravalent cHD37 might <u>not</u> be more effective in mice, it should be superior to the divalent MAb in humans. This may be due to the species of cells that carry out the effector functions in mice; MAbs with human Fc regions effectively mediate secondary effector functions with human NK cells, but not with mouse NK cells. Hence, preclinical studies in mice may not accurately predict their anti-tumor activity in humans.

## B. cHD37-DcVV is More Effective than the Murine HD37 or cHD37 at Mediating Secondary Effector Functions *In Vitro* with Human Effector Cells and Complement

*Binding Affinity of HD37 MAbs*

The clinical utility of an antibody depends on its affinity for the target antigen. Improving affinity can improve the potency and reduce the number of doses needed[130]. In this study, cHD37-DcVV was constructed with four antigen binding sites to improve its binding avidity to CD19. This tetravalent MAb was then compared to the divalent MAbs. Surface plasmon resonance (SPR) (Biacore) is often used to determine the affinity and kinetic rate constants of an antibody-antigen interaction[131]. However, soluble CD19 antigen was not available to test this. Therefore, the relative binding affinity and dissociation of the antibody to human pre-B ALL and Burkitt's lymphoma cell lines expressing low and high densities of CD19, respectively, were evaluated by FACS analysis, Scatchard analysis, and dissociation curves to determine the persistence of the MAbs on the cell surface.

The results of this study indicate that increasing the valency of the antibody did indeed improve its avidity of binding to the target antigen.

cHD37-DcVV has more than two sites that bind antigen simultaneously, and this multivalency contributes to the increased relative binding affinity and the slower off-rate from cells. Therefore the potency, or the anti-tumor efficacy, of the tetravalent cHD37 should be better than that of the divalent cHD37. The *in vitro* experiments were designed to test the effector functions of these MAbs.

*Fc Effector Functions*

One of the most important factors in determining the *in vivo* activity of therapeutic MAbs is the efficient interaction with cellular Fc-receptors on effector cells as well as the binding of complement proteins[25]. In fact, the primary mechanism of action of most therapeutic MAbs such as Rituxan™, Campath™, and Herceptin™ in cancer therapy, is through the recruitment of secondary effector mechanisms including ADCC and CDC[36, 49, 128, 132]. Therapeutic antibodies, including HD37, typically use human IgG1 constant regions because of the capacity of human Fc to induce strong ADCC and CDC effector functions in humans[133]. In an ADCC reaction, MAbs bound to tumor cells through an antigen specific interaction recruit effector cells expressing FcRs that are specific for the Fc region of the MAb. This binding then triggers the release of

inflammatory mediators and cytotoxic substances by the effector cells resulting in the death and eventual clearance of the tumor target cell[25]. In CDC, MAbs bound to tumor cells bind the complement protein C1q, which initiates the complement activation cascade and results in the lysis of the tumor cell through the formation of the membrane attack complex (MAC)[134]. Hence, the specific interactions of the Fc of a MAb with the FcR on effector cells or the C1q protein are important for anti-tumor activity. Initial experiments designed to test the cytotoxic effects of the HD37 MAbs in the absence of effector cells and complement indicated that the MAbs did not inhibit tumor cell growth or the induction of apotosis. Therefore, these results led to the *in vitro* experiments to study the Fc-dependent effector mechanisms of the MAbs including their ability to mediate ADCC and CDC in the presence of both human and murine effector cells and human and murine complement. Taken together, these studies were therefore designed to elucidate the mechanisms of action of divalent and tetravalent cHD37 and to determine if valency affected anti-tumor activity.

*ADCC*

Therapeutic MAbs are typically chimerized to decrease immunogenicity and to optimize their effector functions[27, 31]. The primary

effector cells that mediate ADCC are NK cells[135, 136]. Human NK cells express the activating FcR, FcγRIII, that efficiently binds the human but not the murine Fc region of IgG[106]. Since the cHD37 MAbs are human IgG1s, it was important to assess their ability to mediate effector functions with human effector cells. Previous reports have shown that although murine and human IgG1 bind murine FcγRIII[108-112] comparably well, murine IgG1 binds poorly to human FcγRIII[118, 119]. Therefore, it was not surprising that our results showed that cHD37 MAbs, but not murine HD37, were able to mediate ADCC with human NK cells. Furthermore, murine FcγRIII bind to both mouse and human IgG1[106]. Therefore, all three HD37 MAbs were able to mediate ADCC with murine LAK effector cells.

The ADCC experiments also examined the relationship between the valency of a MAb and its anti-tumor efficacy. The tetravalent cHD37 not only showed an increased relative binding affinity and a slower off-rate from cells as compared to the divalent MAbs, but was also more effective in mediating ADCC when human effector cells were used. However, the caveat is that this increased anti-tumor activity was only observed with human effector cells, but not with murine effector cells. Therefore, there may <u>not</u> be a difference in the anti-tumor efficacy of the tetravalent *versus*

divalent chimeric MAbs in mice and this was supported by the results of our *in vivo* experiments.

Another factor that might affect the efficacy an antibody in mediating effector functions could be related to the difference in internalization by tumor cells. Previous studies comparing the activities and characteristics of homodimers *versus* monomers of HD37 have shown that Daudi cells internalized larger amounts of the former[98]. It was hypothesized that the slower dissociation rate of the homodimer might account for this. However, recent preliminary results have shown that the tetravalent cHD37 has a significantly lower rate of internalization than divalent cHD37 despite the fact that the tetravalent MAb has a slower dissociation rate. This contradiction remains to be explained and might be related to the larger size of the homodimer versus the tetravalent cHD37.

*CDC*

Another important effector function of therapeutic MAbs is the activation of the complement cascade to lyse tumor cells. Previous studies have shown that MAbs such as Rituxan[137], SGN-70, a chimeric anti-CD70 IgG1 MAb for the treatment of lymphomas and multiple myeloma[138], and cA2 G1, a chimeric anti-TNF-α (transmembrane form) IgG1 MAb for the

treatment of rheumatoid arthritis can mediate both ADCC and CDC[139]. Further studies using C1q deficient mice have even suggested that CDC is the primary mechanism of action of Rituxan™ and other anti-CD20 MAbs, and that complement activation has a significant impact on their therapeutic activity[140].

Our study assessed the ability of the cHD37 *versus* murine HD37 to mediate CDC against pre-B ALL and Burkitt's lymphoma tumor cells *in vitro* using mouse or human serum as a source of complement. None of the HD37 MAbs was able to mediate CDC when mouse serum was used as a source of complement. It is not surprising that the cHD37 MAbs were not able to mediate CDC with mouse complement since human IgG1 does not bind mouse C1q[141]. Surprisingly, when human serum was used as a source of complement, divalent cHD37 was not able to mediate CDC either. In contrast, tetravalent cHD37 was able to mediate CDC against Daudi, but not NALM-6 cells. These results suggest that only the tetravalent cMAb can mediate CDC, but only against certain tumor cell lines. In this regard, previous studies have also demonstrated that there is a significant degree of heterogeneity in Rituxan™-mediated CDC when different cell lines were used[49, 120, 142]. This phenomenon has been attributed to the heterogeneous expression of the CD20 molecule on the surface of different lymphoma lines as well as the heterogeneous

expression of the complement inhibitiors CD55 and CD59[120]. Inhibition of these surface molecules increases the ability of Rituxan™ to activate complement and lyse tumor cells. Therefore, differential expression of CD19, CD55, and CD59 on Daudi and NALM-6 cells may be the reason that chimeric tetravalent HD37 can mediate CDC with only Daudi cells. However, further studies must be carried out to confirm this and to study the expression of CD55 and CD59 on the two cell lines.

The ability of the tetravalent, but not the divalent cHD37, to mediate CDC suggests that the valency of the antibody is important in complement activation. This may be due to the slower off-rate (longer $T_{1/2}$ of dissociation) of the tetravalent cHD37 compared to the divalent murine or chimeric MAbs. Hence, a slow dissociation rate might enable the tetravalent cHD37 to activate the complement cascade more efficiently. These results again support the notion that increased valency can increase the anti-tumor potency of a therapeutic MAb, and that this might give tetravalent cHD37 an advantage over the divalent chimeric MAbs in humans.

**C. cHD37-DcVV Could Be Superior to Murine HD37 and cHD37 in Humans**

The *in vitro* data show that the chimeric tetravalent HD37 MAb has a higher relative binding affinity and a slower off rate (longer $T_{1/2}$ of dissociation) than the divalent MAbs, indicating that the tetravalent chimeric MAb is functionally multivalent (more than two of its sites can bind simultaneously). Furthermore, the *in vitro* studies suggest that increased valency translates to better anti-tumor activity. While all three MAbs were able to mediate ADCC when murine effector cells were used, the tetravalent chimeric MAb was more effective than the divalent murine or chimeric MAbs at mediating ADCC and only the tetravalent chimeric MAb was able to mediate CDC in the presence of human complement. These data suggest that the tetravalent chimeric MAb should be more efficacious in humans. Therefore, based on the *in vitro* data alone, the clinical potential of the tetravalent chimeric MAb should be superior. Clinical trials in humans will be necessary to confirm this prediction.

## D. HD37 MAbs Are Equally Effective at Extending the Mean Survival Time of SCID Mice with Human Pre-B ALL and Burkitt's Lymphoma Tumors

*Pharmacokinetics of the HD37 MAbs In Vivo*

The pharmacokinetic properties of MAbs are important in assessing their clinical potential. In the case of "naked" or unconjugated therapeutic MAbs, the goal is to increase the half-life of the MAb to improve efficacy. Serum persistence of MAbs depends on the salvage receptor, FcRn, which rescues IgG from degradation[143-145]. In this study, the *Pk*s of the HD37 MAbs were evaluated in 6-8 week old female Swiss Webster mice. The $T_{1/2}$, bioavailability, and catabolic rate of the HD37 MAbs were all comparable. These results are in accordance with previous studies indicating that the mouse FcRn binds mouse and human IgG1 with relatively comparable affinities (2.4 fold difference between the $R_{eq}$ of hIgG1-mFcRn *versus* mIgG1-mFcRn) as compared to the affinities of human FcRn to mouse and human IgG1 (417 fold difference between the $R_{eq}$ of hIgG1-hFcRn *versus* mIgG1-hFcRn)[123]; therefore, the half-lives of the murine *versus* cHD37 MAbs, should be, and were, similar in mice. In humans, the cHD37 MAbs should have significantly longer half-lives than

the murine MAb because it has been shown that human FcRn binds human IgG1 well and mouse IgG1 very poorly[123]. As a result, studies in mice may not yield a valid prediction of the pharmacokinetic behavior of therapeutic MAbs in humans.

*Precursor B Cell Acute Lymphoblastic Leukemia*

Pre-B ALLs are immature B cell tumors and the treatment regimen consists of radiation and chemotherapy with general immunosuppression as an anticipated consequence[146]. Currently, there are no FDA approved MAbs for the immunotherapy of pre-B ALL even though thousands of children and adults in the United States are diagnosed with this type of cancer every year. Previous studies in our lab have shown that HD37 conjugated to dgRTA in combination with either an anti-CD22 MAb conjugated to dgRTA or chemotherapy significantly improved the survival of SCID mice with disseminated human pre-B ALL tumor cell lines[91, 92]. Pre-B ALLs express CD19 at varying levels[68, 86]. An anti-CD19 MAb that has reduced systemic toxicity compared to chemotherapy and is efficacious against tumors with varying levels of CD19 surface expression would be an ideal immunotherapy for pre-B ALLs.

One of the goals of this study was to determine whether the HD37 MAbs were effective in the treatment of tumors with varying densities of CD19 surface expression. Therefore, both $CD19^{lo}$ (NALM-6) and $CD19^{hi}$ (Daudi) tumor cell lines were tested. Murine HD37, cHD37 and tetravalent cHD37 were evaluated in 6-8 week old female SCID mice with a $CD19^{lo}$ human pre-B ALL tumors. In such studies, all three MAbs prolonged survival in mice with disseminated disease as compared to the isotype-matched control. In these experiments, the murine and cHD37 were administered at a dose of 7.5 µg/g mouse (22.6 $mg/m^2$ human equivalent) on each of four consecutive days (90.4 $mg/m^2$ total). The tetravalent cHD37 was administered at an equivalent molar dose of $5 \times 10^{-11}$ M/g, or 10 µg/g mouse also on each of four consecutive days. Dosage and administration was chosen based on previous *in vivo* experiments with murine HD37[87, 94]. The use of unconjugated monoclonal antibody therapy for hematological malignancies in humans is usually carried out at doses much higher than those used in this study. For example, Campath™, an anti-CD52 MAb for the treatment of B-CLL, is administered at 1168.6 $mg/m^2$ weekly[54]; Rituxan™, an anti-CD20 MAb for NHL, is administered at 375 $mg/m^2$ every 3 weeks for previously untreated disease or weekly for refractory disease[45]; lumiliximab (in clinical trials), an anti-CD23 MAb for CLL, is administered at 500 $mg/m^2$ weekly[147]; and epratuzamab (in clinical

trials), an anti-CD22 for NHL, is administered at 360 mg/m$^2$ weekly[148]. In one particular clinical trial, patients with NHL were treated with a mouse IgG2a anti-CD19 MAb at doses of 8764 – 38953 mg/m$^2$, over 386 times greater than the dose that was administered in this study. In conclusion, these data show that while all three HD37 MAbs were effective in the treatment of a CD19$^{lo}$ expressing pre-B ALL tumor, higher doses of the HD37 MAbs should be even more effective in treating pre-B ALL. Unfortunately, we could not generate the quantities of MAbs necessary to test this.

*Burkitt's Lymphoma*

Burkitt's lymphoma is a type of B cell NHL. A Burkitt's lymphoma, Daudi, was chosen for this study because previous studies have shown that Daudi cells highly and stably express CD19 on their surface[149]. In addition, murine HD37 has been shown to have anti-tumor activity against Daudi tumors in SCID mice[87].

NHLs are a heterogeneous group of cancers of B cell origin, and the treatment options vary according to NHL type and stage though often involving a combination of chemotherapy, radiation therapy, and hematopoietic stem cell transplant[150]. In the last decade antibody

therapies targeting CD20 (Rituxan™ and the radioimmunoconjugates Bexxar™ and Zevalin™) have demonstrated activity with comparatively reduced systemic toxicity in patients with B cell NHLs[48, 148, 151]. CD19 is also expressed on most B cell NHL[68, 86]. Therefore, HD37 is an attractive immunotherapy for patients who are refractory to anti-CD20 therapy, have tumors that do not express CD20 but express CD19, or tumors that have lost CD20 expression following multiple rounds of anti-CD20 immunotherapy.

All three HD37 MAbs were equally effective in the treatment of SCID mice with $CD19^{lo}$ pre-B ALL tumors. Therefore, another goal of the *in vivo* studies was to evaluate the efficacy of the chimeric HD37 MAbs against a $CD19^{hi}$ human Burkitt's lymphoma tumor, and to determine whether there was a correlation between the valency of the chimeric HD37 MAbs and the therapeutic dose required for optimal anti-tumor activity in SCID mice. SCID mice with human Burkitt's lymphoma were treated with 7.5, 3.8, or 1.9 µg/g mouse of cHD37 or the molar equivalent of cHD37-DcVV (10, 5, or 2.5 µg/g mouse). At lower levels of MAb, as compared to saturated levels of MAb, there may be a difference between the efficacies of the divalent and the tetravalent cMAbs. However, the results showed that although the divalent and tetravalent cHD37 prolonged the mean survival times of the SCID mice with the $CD19^{hi}$ human Burkitt's

lymphoma cells as compared to the isotype-matched control, there was no difference between treatment with cHD37 and cHD37-DcVV even at the equivalent lower doses.

These data, together with the data from the *in vivo* pre-B ALL tumor model, suggest that the difference between efficacies of the chimeric *versus* the murine HD37 and the divalent *versus* the tetravalent cHD37 cannot be accurately determined in SCID mice with human tumors. An alternative mouse model that might better differentiate the anti-tumor activities between murine HD37 and cHD37, and between cHD37 and tetravalent cHD37 is a SCID mouse with transgenic human FcγRI and FcγIII[152, 153]. As previously discussed, murine FcγRI and FcγRIII bind both human and murine IgG1, but human FcγRI and FcγRIII only bind human IgG1. The *in vitro* assays also showed that there was a difference in the activities of the divalent *versus* tetravalent MAbs when human *versus* mouse effector cells were used. Therefore, SCID mice expressing human FcγRI and FcγIII on their myeloid cells will be useful in the *in vivo* studies. To eliminate ambiguity, these SCID mice should also be murine FcγR-deficient (or $Fc\gamma^{-/-}$)[154]. However, previous studies have shown that while the immunoreceptor tyrosine-based activation motif (ITAM)-accessory chain-associated activating FcγRs, such as FcγRI and FcγRIII, are important in the anti-tumor activity of MAbs, the immunoreceptor tyrosine-

based inhibition motif (ITIM)-containing inhibitory receptor, FcγRIIb, is involved in regulating MAb activity by downregulating anti-tumor activity[36]. Rituxan™ and Herceptin™ have an increased ability to kill xenogeneic tumor cells in mice lacking FcγRII, the murine homolog of human FcγRIIb. Therefore, SCID mice deficient in murine FcγRs and transgenic for the expression of both activating human FcγRs, FcγRI and FcγRIII, and the inhibitory human FcγRIIb receptor would be a more ideal model to study the anti-tumor activities of the HD37 MAbs.

**E. Preclinical Studies in Mouse Models May Not Accurately Predict MAb Activity in Humans**

Chimerizing and humanizing naked antibodies using recombinant DNA technology is important in reducing the immunogenicity and improving their *Pk* and effector functions of MAbs designed for clinical use in humans, particularly for the treatment of cancer. Unfortunately, chimeric and human MAbs are difficult to evaluate in mice[155]. In particular, immunogenicity, pharmacokinetics and the interaction with the host immune system are affected once an antibody is chimerized or humanized, and studies to test these changes can only be done in humans or transgenic mice, many of which are not yet available. However, mice are required by the FDA to test the MAbs before the approval for use in humans. Therefore, the results from animal studies must be critically assessed for their limitations since none of the available animal models are able to fully mimic the situation in patients.

One dramatic example of the discrepancy between the results from preclinical animal studies and the resulting consequence in humans is the anti-CD28 superagonist TGN1412. Preclinical studies showed promising results in the effective therapy for experimental autoimmune

encephalomyelitis in mice[156]. However, in ensuing clinical trials, cytokine storm was elicited in six patients receiving the MAb therapy[157]. Of course not all MAb therapy development studies had such unfortunate results. Some antibodies such as Rituxan™[137] and Herceptin™[158] are highly effective in humans. Extensive preclinical studies of both MAbs in animal models have validated their anti-tumor efficacy[137, 159]. Their pharmacokinetics and mechanisms of action have been elucidated in animal studies, and the data have been used to translate the clinical activity of the MAbs[160]. Yet, even with these antibodies preclinical studies in animals did not always accurately predict the activity of some MAbs such as Rituxan™ and Herceptin™ in humans. For example, one study using xenografted mice indicated that ADCC was the predominant mechanism of action of both MAbs[36]. However, clinical studies in patients indicate that Rituxan™ induces apoptosis in tumor cells via the caspase-9 pathway[161]. Preclinical studies in mice also showed that the half-life of Herceptin™ was approximately 7 days, while in humans, the half-life is approximately 21 days[160]. These examples illustrate the limitations of preclinical studies in mice and perhaps suggest that more emphasis should be placed on *in vitro* data using human cells and sera.

In the case of the HD37 MAbs, there are already indications from this study that the activity of the cHD37 MAbs, and in particular the

tetravalent MAb in humans, will be quite different from their behavior in mice. Thus, although the *Pk*s of all three MAbs are comparable, *Pk* studies are performed in mice bearing murine FcRns, which determine the persistence of a MAb in the body. As previously reported, murine FcRns and human FcRns bind mouse and human IgG differently[123]. Therefore, although the preclinical studies show that all three MAbs have comparable *Pk*s, the prediction is that the chimeric MAbs will have longer half-lives and better *Pk*s in humans than murine HD37. A more useful model in determining the *Pk*s of the cHD37 MAbs would one which uses mice expressing human FcRns and lacking endogenous murine FcRns[162]. In one study, engineered humanized IgG1 MAbs had significantly longer $T_{1/2}$s in these hFcRn transgenic mice than in mice bearing endogenous FcRn[162]. These results indicate that transgenic hFcRn mice are a promising surrogate for human IgG therapeutic development.

Immunodeficient mice are particularly useful as hosts for the propagation of xenografts, which can be derived from cell lines, since these mice do not reject human tumors[155]. In this study, SCID with human pre-B ALL or Burkitt's lymphoma tumors were used to assess the anti-tumor efficacy of the HD37 MAbs. SCID mice are devoid of T and B cells, but do have effector cells including monocytes, granulocytes and NK cells[163, 164]. Because these cells are of murine origin, their interaction with

MAbs bearing human Fc regions may not accurately reflect the interaction of the human effector cells with human MAbs. The data from the *in vitro* and *in vivo* experiments in this study suggest that the anti-tumor efficacy of the tetravalent MAb may be more effective in humans, but the difference in the anti-tumor activties of the three MAbs is not apparent in SCID mice. In mice, not only are the numbers of FcγRs different but so are their expression and functions. Therefore preclinical studies using human MAbs in mice do not necessarily translate into similar effects in humans. Hence, the interpretation of the *in vivo* data from this study must be taken in context with the *in vitro* data.

In summary, future studies examining the potential anti-tumor activities of an antibody (or any agent) should continue to be evaluated in animals because of the importance of demonstrating the activity and safety of the agent in non-human primates. However, as this study and the previous study with the MAb against CD28 (TGN1412) have demonstrated, it is important to carefully evaluate *in vitro* data using human cells since no animal model is able to completely mimic the behavior of any MAb in humans. Furthermore, it is also important to carefully understand the differences between human and animal Fc receptors and their interactions with their ligands. In extreme cases, such as in the case of TGN1412[157], the species difference between

receptor/ligand interactions can mean a dampened response (in mice) or heightened activation leading to cytokine storm (in humans). In the study reported here, comparing the activities of a mouse *versus* human and divalent *versus* tetravalent cHD37 MAbs would clearly benefit from a mouse model where the FcRs and effector cells were of human origin.

**F. Conclusions.**

Several therapeutic MAbs have excellent anti-cancer activity and have become important treatment options, either alone or in combination with other modalities. Many MAbs have already been FDA-approved for the treatment of a variety of cancers, and their scope is rapidly expanding. MAbs are a valuable treatment option due to their ability to target antigens specifically expressed or up-regulated on tumor cells, and reduced toxicity and adverse effects. MAbs can also be manipulated to have increased anti-tumor activity while minimizing any adverse cytotoxic effects.

The objectives of this study were to construct, express, and test the *in vitro* and *in vivo* activities of divalent and tetravalent cHD37 with the goal of using these data to determine which chimeric MAb to move forward into clinical trials. The activities of the two cHD37 MAbs were compared to each other as well as to that of the murine MAb. Although all three HD37 MAbs were equally effective at extending the mean survival time of SCID mice with human pre-B ALL and Burkitt's lymphoma tumors, the tetravalent cHD37 was more effective than the murine and divalent chimeric MAbs at mediating secondary effector functions *in vitro* with human effector cells and complement. These findings suggest that the tetravalent cHD37 should be superior to the divalent cHD37 in humans,

and that preclinical studies in mice may not accurately predict the activity of these MAbs in humans. Further studies need to be performed in animal models that better mimic the human system to elucidate the *in vivo* activities of the cMAbs and determine whether there is a correlation between the valency and the anti-tumor potency of the MAbs. Clinical trials will therefore be critical in assessing the potential of engineered MAbs in cancer patients.

## REFERENCES


1. US Cancer Statistics Working Group. United States Cancer Statistics: 1999-2005 Incidence and Mortality Web-based Report *Department of Health and Human Services, Centers for Disease Control and Prevention, and National Cancer Institute*, Atlanta, GA, (2009) www.cdc.giv/uscs

2. Pui, C.H., Robison, L.L. & Look, A.T. Acute lymphoblastic leukaemia. *Lancet* **371**, 1030-43 (2008).

3. American Cancer Society. Cancer Facts and Figures 2008. *American Cancer Society,* Atlanta, GA (2008) www.cancer.gov

4. Xie, Y., Davies, S.M., Xiang, Y., Robison, L.L. & Ross, J.A. Trends in leukemia incidence and survival in the United States (1973-1998). *Cancer* **97**, 2229-35 (2003).

5. Ries, L.A.G. et al. SEER Cancer Statistics Review, 1975-2005 (National Cancer Institute NIH, Bethesda, MD, 2007).

6. Moricke, A. et al. Risk-adjusted therapy of acute lymphoblastic leukemia can decrease treatment burden and improve survival: treatment results of 2169 unselected pediatric and adolescent patients enrolled in the trial ALL-BFM 95. *Blood* **111**, 4477-89 (2008).

7. Whitlock, J.A. Down syndrome and acute lymphoblastic leukaemia. *Br J Haematol* **135**, 595-602 (2006).

8. Hasle, H. Pattern of malignant disorders in individuals with Down's syndrome. *Lancet Oncol* **2**, 429-36 (2001).

9. Yagi, T. et al. Detection of clonotypic IGH and TCR rearrangements in the neonatal blood spots of infants and children with B-cell precursor acute lymphoblastic leukemia. *Blood* **96**, 264-8 (2000).

10. Taub, J.W. et al. High frequency of leukemic clones in newborn screening blood samples of children with B-precursor acute lymphoblastic leukemia. *Blood* **99**, 2992-6 (2002).

11. Pui, C.H. & Evans, W.E. Treatment of acute lymphoblastic leukemia. *N Engl J Med* **354**, 166-78 (2006).

12. Chabner, B.A. & Roberts, T.G., Jr. Timeline: Chemotherapy and the war on cancer. *Nat Rev Cancer* **5**, 65-72 (2005).

13. Pileri, S.A., Milani, M., Fraternali-Orcioni, G. & Sabattini, E. From the R.E.A.L. Classification to the upcoming WHO scheme: a step toward universal categorization of lymphoma entities? *Ann Oncol* **9**, 607-12 (1998).

14. Rogers, B.B. Overview of non-Hodgkin's lymphoma. *Semin Oncol Nurs* **22**, 67-72 (2006).

15. Kohler, G. & Milstein, C. Continuous cultures of fused cells secreting antibody of predefined specificity. *Nature* **256**, 495-7 (1975).

16. Schrama, D., Reisfeld, R.A. & Becker, J.C. Antibody targeted drugs as cancer therapeutics. *Nat Rev Drug Discov* **5**, 147-59 (2006).

17. von Mehren, M., Adams, G.P. & Weiner, L.M. Monoclonal antibody therapy for cancer. *Annu Rev Med* **54**, 343-69 (2003).

18. Schwartz, R.S. Paul Ehrlich's magic bullets. *N Engl J Med* **350**, 1079-80 (2004).

19. Trauth, B.C. et al. Monoclonal antibody-mediated tumor regression by induction of apoptosis. *Science* **245**, 301-5 (1989).

20. Waldmann, T.A. Monoclonal antibodies in diagnosis and therapy. *Science* **252**, 1657-62 (1991).

21. Egen, J.G., Kuhns, M.S. & Allison, J.P. CTLA-4: new insights into its biological function and use in tumor immunotherapy. *Nat Immunol* **3**, 611-8 (2002).

22. Sanderson, K. et al. Autoimmunity in a phase I trial of a fully human anti-cytotoxic T-lymphocyte antigen-4 monoclonal antibody with multiple melanoma peptides and Montanide ISA 51 for patients with resected stages III and IV melanoma. *J Clin Oncol* **23**, 741-50 (2005).

23. Genentech, Inc. Avastin (bevacizumab): Reach beyond convention. (2008) www.avastin.com

24. Imclone Systems, Inc., Bristol-Myers Squibb Co., Merck, Inc. Erbitux (cetuximab). (2008) www.erbitux.com

25. Nimmerjahn, F. & Ravetch, J.V. Antibodies, Fc receptors and cancer. *Curr Opin Immunol* **19**, 239-45 (2007).

26. Ravetch, J.V. Fc receptors *in Fundamental Immunology 5$^{th}$ edition* (ed. Paul, W.E.) (Lippincott Williams & Wilkins, Philadelphia, PA, 2003).

27. Morrison, S.L., Johnson, M.J., Herzenberg, L.A. & Oi, V.T. Chimeric human antibody molecules: mouse antigen-binding domains with human constant region domains. *Proc Natl Acad Sci U S A* **81**, 6851-5 (1984).

28. Ward, E.S. & Ghetie, V. The effector functions of immunoglobulins: implications for therapy. *Ther Immunol* **2**, 77-94 (1995).

29. Isaacs, J.D., Clark, M.R., Greenwood, J. & Waldmann, H. Therapy with monoclonal antibodies. An in vivo model for the assessment of therapeutic potential. *J Immunol* **148**, 3062-71 (1992).

30. Carter, P. Improving the efficacy of antibody-based cancer therapies. *Nat Rev Cancer* **1**, 118-29 (2001).

31. Boulianne, G.L., Hozumi, N. & Shulman, M.J. Production of functional chimaeric mouse/human antibody. *Nature* **312**, 643-6 (1984).

32. Jones, P.T., Dear, P.H., Foote, J., Neuberger, M.S. & Winter, G. Replacing the complementarity-determining regions in a human antibody with those from a mouse. *Nature* **321**, 522-5 (1986).

33. Hwang, W.Y. & Foote, J. Immunogenicity of engineered antibodies. *Methods* **36**, 3-10 (2005).

34. Jakobovits, A. et al. Germ-line transmission and expression of a human-derived yeast artificial chromosome. *Nature* **362**, 255-8 (1993).

35. Clynes, R., Takechi, Y., Moroi, Y., Houghton, A. & Ravetch, J.V. Fc receptors are required in passive and active immunity to melanoma. *Proc Natl Acad Sci U S A* **95**, 652-6 (1998).

36. Clynes, R.A., Towers, T.L., Presta, L.G. & Ravetch, J.V. Inhibitory Fc receptors modulate in vivo cytoxicity against tumor targets. *Nat Med* **6**, 443-6 (2000).

37. Shields, R.L. et al. High resolution mapping of the binding site on human IgG1 for Fc gamma RI, Fc gamma RII, Fc gamma RIII, and

FcRn and design of IgG1 variants with improved binding to the Fc gamma R. *J Biol Chem* **276**, 6591-604 (2001).

38. Wright, A. & Morrison, S.L. Effect of glycosylation on antibody function: implications for genetic engineering. *Trends Biotechnol* **15**, 26-32 (1997).

39. Lifely, M.R., Hale, C., Boyce, S., Keen, M.J. & Phillips, J. Glycosylation and biological activity of CAMPATH-1H expressed in different cell lines and grown under different culture conditions. *Glycobiology* **5**, 813-22 (1995).

40. Umana, P., Jean-Mairet, J., Moudry, R., Amstutz, H. & Bailey, J.E. Engineered glycoforms of an antineuroblastoma IgG1 with optimized antibody-dependent cellular cytotoxic activity. *Nat Biotechnol* **17**, 176-80 (1999).

41. Idusogie, E.E. et al. Engineered antibodies with increased activity to recruit complement. *J Immunol* **166**, 2571-5 (2001).

42. Li, B. et al. Development of novel tetravalent anti-CD20 antibodies with potent antitumor activity. *Cancer Res* **68**, 2400-8 (2008).

43. Meng, R. et al. The evaluation of recombinant, chimeric, tetravalent antihuman CD22 antibodies. *Clin Cancer Res* **10**, 1274-81 (2004).

44. Farah, R.A., Clinchy, B., Herrera, L. & Vitetta, E.S. The development of monoclonal antibodies for the therapy of cancer. *Crit Rev Eukaryot Gene Expr* **8**, 321-56 (1998).

45. Genentech, Inc. and Biogen IDEC. Rituxan (rituximab): Targeted B Cell Therapy (2008) www.rituxan.com

46. Stashenko, P., Nadler, L.M., Hardy, R. & Schlossman, S.F. Characterization of a human B lymphocyte-specific antigen. *J Immunol* **125**, 1678-85 (1980).

47. Press, O.W., Howell-Clark, J., Anderson, S. & Bernstein, I. Retention of B-cell-specific monoclonal antibodies by human lymphoma cells. *Blood* **83**, 1390-7 (1994).

48. Coiffier, B. Rituximab therapy in malignant lymphoma. *Oncogene* **26**, 3603-13 (2007).

49. Harjunpaa, A., Junnikkala, S. & Meri, S. Rituximab (anti-CD20) therapy of B-cell lymphomas: direct complement killing is superior to cellular effector mechanisms. *Scand J Immunol* **51**, 634-41 (2000).

50. GlaxoSmithKline, Inc. Bexxar (tositumomab and Iodine 131 tositumomab). (2008) www.bexxar.com

51. Cell Therapeutics, Inc. Zevalin (ibritumomab tiuxetan). (2008) www.zevalin.com

52. Stanglmaier, M., Reis, S. & Hallek, M. Rituximab and alemtuzumab induce a nonclassic, caspase-independent apoptotic pathway in B-lymphoid cell lines and in chronic lymphocytic leukemia cells. *Ann Hematol* **83**, 634-45 (2004).

53. Golay, J., Manganini, M., Rambaldi, A. & Introna, M. Effect of alemtuzumab on neoplastic B cells. *Haematologica* **89**, 1476-83 (2004).

54. Genzyme Corporation, Bayer Healthcare Pharmaceuticals Inc. Campath for the Treatment of B-Cell Chronic Lymphocytic Leukemia. (2008) www.campath.com

55. Alinari, L. et al. Alemtuzumab (Campath-1H) in the treatment of chronic lymphocytic leukemia. *Oncogene* **26**, 3644-53 (2007).

56. Ravandi, F. & O'Brien, S. Alemtuzumab in CLL and other lymphoid neoplasms. *Cancer Invest* **24**, 718-25 (2006).

57. Wendtner, C.M. et al. Consolidation with alemtuzumab in patients with chronic lymphocytic leukemia (CLL) in first remission--experience on safety and efficacy within a randomized multicenter phase III trial of the German CLL Study Group (GCLLSG). *Leukemia* **18**, 1093-101 (2004).

58. Montillo, M. et al. Alemtuzumab as consolidation after a response to fludarabine is effective in purging residual disease in patients with chronic lymphocytic leukemia. *J Clin Oncol* **24**, 2337-42 (2006).

59. Tedder, T.F. & Isaacs, C.M. Isolation of cDNAs encoding the CD19 antigen of human and mouse B lymphocytes. A new member of the immunoglobulin superfamily. *J Immunol* **143**, 712-7 (1989).

60. Chalupny, N.J. et al. Specific binding of Fyn and phosphatidylinositol 3-kinase to the B cell surface glycoprotein CD19 through their src homology 2 domains. *Eur J Immunol* **25**, 2978-84 (1995).

61. Tuveson, D.A., Carter, R.H., Soltoff, S.P. & Fearon, D.T. CD19 of B cells as a surrogate kinase insert region to bind phosphatidylinositol 3-kinase. *Science* **260**, 986-9 (1993).

62. Uckun, F.M. et al. Signal transduction through the CD19 receptor during discrete developmental stages of human B-cell ontogeny. *J Biol Chem* **268**, 21172-84 (1993).

63. Weng, W.K., Jarvis, L. & LeBien, T.W. Signaling through CD19 activates Vav/mitogen-activated protein kinase pathway and induces formation of a CD19/Vav/phosphatidylinositol 3-kinase complex in human B cell precursors. *J Biol Chem* **269**, 32514-21 (1994).

64. Bradbury, L.E., Goldmacher, V.S. & Tedder, T.F. The CD19 signal transduction complex of B lymphocytes. Deletion of the CD19 cytoplasmic domain alters signal transduction but not complex formation with TAPA-1 and Leu 13. *J Immunol* **151**, 2915-27 (1993).

65. Zhou, L.J., Ord, D.C., Hughes, A.L. & Tedder, T.F. Structure and domain organization of the CD19 antigen of human, mouse, and guinea pig B lymphocytes. Conservation of the extensive cytoplasmic domain. *J Immunol* **147**, 1424-32 (1991).

66. Matsumoto, A.K. et al. Functional dissection of the CD21/CD19/TAPA-1/Leu-13 complex of B lymphocytes. *J Exp Med* **178**, 1407-17 (1993).

67. Fearon, D.T. & Carroll, M.C. Regulation of B lymphocyte responses to foreign and self-antigens by the CD19/CD21 complex. *Annu Rev Immunol* **18**, 393-422 (2000).

68. Scheuermann, R.H. & Racila, E. CD19 antigen in leukemia and lymphoma diagnosis and immunotherapy. *Leuk Lymphoma* **18**, 385-97 (1995).

69. Dorken, B., Moller, P., Pezzutto, A., Schwartz-Albeiz, R. & Moldenhauer, G. B2 B Cell Antigens: CD19 *in Leukocyte Typing IV - White Cell Differentiation Antigens* (ed. Knapp, D., Gilks, Rieber, Schmitt, Stein, von dem Borne) pg 34-36 (Oxford University Press, Oxford, 1998).

70. Carter, R.H., Tuveson, D.A., Park, D.J., Rhee, S.G. & Fearon, D.T. The CD19 complex of B lymphocytes. Activation of phospholipase C by a protein tyrosine kinase-dependent pathway that can be enhanced by the membrane IgM complex. *J Immunol* **147**, 3663-71 (1991).

71. Chalupny, N.J. et al. Tyrosine phosphorylation of CD19 in pre-B and mature B cells. *EMBO J* **12**, 2691-6 (1993).

72. Bradbury, L.E., Kansas, G.S., Levy, S., Evans, R.L. & Tedder, T.F. The CD19/CD21 signal transducing complex of human B lymphocytes includes the target of antiproliferative antibody-1 and Leu-13 molecules. *J Immunol* **149**, 2841-50 (1992).

73. Kansas, G.S. & Tedder, T.F. Transmembrane signals generated through MHC class II, CD19, CD20, CD39, and CD40 antigens induce LFA-1-dependent and independent adhesion in human B cells through a tyrosine kinase-dependent pathway. *J Immunol* **147**, 4094-102 (1991).

74. Tedder, T.F., Inaoki, M. & Sato, S. The CD19-CD21 complex regulates signal transduction thresholds governing humoral immunity and autoimmunity. *Immunity* **6**, 107-18 (1997).

75. Carter, R.H. & Fearon, D.T. CD19: lowering the threshold for antigen receptor stimulation of B lymphocytes. *Science* **256**, 105-7 (1992).

76. Engel, P. et al. Abnormal B lymphocyte development, activation, and differentiation in mice that lack or overexpress the CD19 signal transduction molecule. *Immunity* **3**, 39-50 (1995).

77. Uckun, F.M. et al. Detailed studies on expression and function of CD19 surface determinant by using B43 monoclonal antibody and the clinical potential of anti-CD19 immunotoxins. *Blood* **71**, 13-29 (1988).

78. Pezzutto, A. et al. Flow cytometry analysis of the B cell blind panel: Joint report *in Leukocyte Typing IV - White Cell Differentiation Antigens* (ed. Knapp, D., Gilks, Rieber, Schmitt, Stein, von dem Borne) pg 165-174 (Oxford University Press, Oxford, 1989).

79. Schwonzen, M. et al. Immunophenotyping of low-grade B-cell lymphoma in blood and bone marrow: poor correlation between immunophenotype and cytological/histological classification. *Br J Haematol* **83**, 232-9 (1993).

80. Robbins, B.A. et al. Diagnostic application of two-color flow cytometry in 161 cases of hairy cell leukemia. *Blood* **82**, 1277-87 (1993).

81. Anderson, K.C. et al. Expression of human B cell-associated antigens on leukemias and lymphomas: a model of human B cell differentiation. *Blood* **63**, 1424-33 (1984).

82. Davis, T.A., Czerwinski, D.K. & Levy, R. Therapy of B-cell lymphoma with anti-CD20 antibodies can result in the loss of CD20 antigen expression. *Clin Cancer Res* **5**, 611-5 (1999).

83. Kennedy, G.A. et al. Incidence and nature of CD20-negative relapses following rituximab therapy in aggressive B-cell non-Hodgkin's lymphoma: a retrospective review. *Br J Haematol* **119**, 412-6 (2002).

84. Haidar, J.H. et al. Loss of CD20 expression in relapsed lymphomas after rituximab therapy. *Eur J Haematol* **70**, 330-2 (2003).

85. Bello, C. & Sotomayor, E.M. Monoclonal antibodies for B-cell lymphomas: rituximab and beyond. *Hematology Am Soc Hematol Educ Program* **2007**, 233-42 (2007).

86. Pezzutto, A. et al. HD37 monoclonal antibody: a useful reagent for further characterization of "non-T/non-B" lymphoid malignancies. (eds. Reinherz, E.L., Haynes, B.F., Nadler, L.M. & Bernstein, I.D.) (Springer-Verlag, Heidelberg/New York, 1986).

87. Ghetie, M.A. et al. Anti-CD19 inhibits the growth of human B-cell tumor lines in vitro and of Daudi cells in SCID mice by inducing cell cycle arrest. *Blood* **83**, 1329-36 (1994).

88. Pezzutto, A. et al. CD19 monoclonal antibody HD37 inhibits anti-immunoglobulin-induced B cell activation and proliferation. *J Immunol* **138**, 2793-9 (1987).

89. Ghetie, M.A. et al. Evaluation of ricin A chain-containing immunotoxins directed against CD19 and CD22 antigens on normal and malignant human B-cells as potential reagents for in vivo therapy. *Cancer Res* **48**, 2610-7 (1988).

90. Herrera, L. et al. Immunotoxins against CD19 and CD22 are effective in killing precursor-B acute lymphoblastic leukemia cells in vitro. *Leukemia* **14**, 853-8 (2000).

91. Herrera, L., Stanciu-Herrera, C., Morgan, C., Ghetie, V. & Vitetta, E.S. Anti-CD19 immunotoxin enhances the activity of chemotherapy in severe combined immunodeficient mice with human pre-B acute lymphoblastic leukemia. *Leuk Lymphoma* **47**, 2380-7 (2006).

92. Herrera, L., Yarbrough, S., Ghetie, V., Aquino, D.B. & Vitetta, E.S. Treatment of SCID/human B cell precursor ALL with anti-CD19 and anti-CD22 immunotoxins. *Leukemia* **17**, 334-8 (2003).

93. Ghetie, M.A., Tucker, K., Richardson, J., Uhr, J.W. & Vitetta, E.S. Eradication of minimal disease in severe combined immunodeficient mice with disseminated Daudi lymphoma using

chemotherapy and an immunotoxin cocktail. *Blood* **84**, 702-7 (1994).

94. Ghetie, M.A., Tucker, K., Richardson, J., Uhr, J.W. & Vitetta, E.S. The antitumor activity of an anti-CD22 immunotoxin in SCID mice with disseminated Daudi lymphoma is enhanced by either an anti-CD19 antibody or an anti-CD19 immunotoxin. *Blood* **80**, 2315-20 (1992).

95. Conry, R.M. et al. Phase I trial of an anti-CD19 deglycosylated ricin A chain immunotoxin in non-Hodgkin's lymphoma: effect of an intensive schedule of administration. *J Immunother Emphasis Tumor Immunol* **18**, 231-41 (1995).

96. Stone, M.J. et al. A phase I study of bolus versus continuous infusion of the anti-CD19 immunotoxin, IgG-HD37-dgA, in patients with B-cell lymphoma. *Blood* **88**, 1188-97 (1996).

97. Messmann, R.A. et al. A phase I study of combination therapy with immunotoxins IgG-HD37-deglycosylated ricin A chain (dgA) and IgG-RFB4-dgA (Combotox) in patients with refractory CD19(+), CD22(+) B cell lymphoma. *Clin Cancer Res* **6**, 1302-13 (2000).

98. Ghetie, M.A. et al. Homodimerization of tumor-reactive monoclonal antibodies markedly increases their ability to induce growth arrest or apoptosis of tumor cells. *Proc Natl Acad Sci U S A* **94**, 7509-14 (1997).

99. Coloma M.J., H.A., Wims L.A., and Morrison S.L. Novel vectors for the expression of antibody molecules using variable regions generated by polymerase chain reaction. *J Immunol Methods* **152**, 89-104 (1992).

100. Kipriyanov S.M., K.O.A., Little M., Moldenhauer G. Rapid detection of recombinant antibody fragments directed against cell-surface antigens by flow cytometry. *J Immunol Methods* **196**, 51-62 (1996).

101. Smallshaw, J., Coleman, E.J., Spiridon, C. & Vitetta, E.S. The Generation and Anti-Myeloma Activity of a Chimeric anti-CD54 Antibody, cUV3. *J Immunother.* **27**, 419-424 (2004).

102. Fraker P. J., a.S.J.C., Jr. Protein and cell membrane iodinations with a sparingly soluble chloramide, 1,3,4,6-tetrachloro-3a,6a-diphenylglycoluril. *Biochem. Biophys. Res. Commun.* **80**, 849-857 (1978).

103. Trucco M., De Petris, S. Determination of equilibrium binding parameters of monoclonal antibodies specific for cell surface antigens *in Immunological Methods, II* (ed. I. Lefkovits and B. Pernis) pg 1-26 (Academic Press, New York, 1981).

104. Coleman E.J., B.K.J., Smallshaw J.E., Vitetta E.S. The Fc Portion of UV3, an Anti-CD54 Monoclonal Antibody, Is Critical for its Antitumor Activity in SCID Mice With Human Multiple Myeloma or Lymphoma Cell Lines. *J Immunother.* **29**, 489-498 (2006).

105. Shumaker, R.C. PKCALC: a BASIC interactive computer program for statistical and pharmacokinetic analysis of data. *Drug Metab Rev.* **17**, 331-348 (1986).

106. Hulett, M.D. & Hogarth, P.M. Molecular basis of Fc receptor function. *Adv Immunol* **57**, 1-127 (1994).

107. Haeffner-Cavaillon, N., Klein, M. & Dorrington, K.J. Studies on the Fc gamma receptor of the murine macrophage-like cell line P388D1. I. The binding of homologous and heterologous immunoglobulin G1. *J Immunol* **123**, 1905-13 (1979).

108. Unkeless, J.C. Characterization of a monoclonal antibody directed against mouse macrophage and lymphocyte Fc receptors. *J Exp Med* **150**, 580-96 (1979).

109. Unkeless, J.C. The presence of two Fc receptors on mouse macrophages: evidence from a variant cell line and differential trypsin sensitivity. *J Exp Med* **145**, 931-45 (1977).

110. Heusser, C.H., Anderson, C.L. & Grey, H.M. Receptors for IgG: subclass specificity of receptors on different mouse cell types and the definition of two distinct receptors on a macrophage cell line. *J Exp Med* **145**, 1316-27 (1977).

111. Teillaud, J.L., Diamond, B., Pollock, R.R., Fajtova, V. & Scharff, M.D. Fc receptors on cultured myeloma and hybridoma cells. *J Immunol* **134**, 1774-9 (1985).

112. Lopez, A.F., Battye, F.L. & Vadas, M.A. Fc receptors on mouse neutrophils and eosinophils: antigenic characteristics, isotype specificity and relative cell membrane density measured by flow cytometry. *Immunology* **55**, 125-33 (1985).

113. Anderson, C.L. Isolation of the receptor for IgG from a human monocyte cell line (U937) and from human peripheral blood monocytes. *J Exp Med* **156**, 1794-806 (1982).

114. Perussia, B., Starr, S., Abraham, S., Fanning, V. & Trinchieri, G. Human natural killer cells analyzed by B73.1, a monoclonal antibody blocking Fc receptor functions. I. Characterization of the lymphocyte subset reactive with B73.1. *J Immunol* **130**, 2133-41 (1983).

115. Jones, D.H., Looney, R.J. & Anderson, C.L. Two distinct classes of IgG Fc receptors on a human monocyte line (U937) defined by differences in binding of murine IgG subclasses at low ionic strength. *J Immunol* **135**, 3348-53 (1985).

116. Van de Winkel, J.G. et al. Characterization of two Fc receptors for mouse immunoglobulins on human monocytes and cell lines. *Scand J Immunol* **26**, 663-72 (1987).

117. Ceuppens, J.L., Baroja, M.L., Van Vaeck, F. & Anderson, C.L. Defect in the membrane expression of high affinity 72-kD Fc gamma receptors on phagocytic cells in four healthy subjects. *J Clin Invest* **82**, 571-8 (1988).

118. Kipps, T.J., Parham, P., Punt, J. & Herzenberg, L.A. Importance of immunoglobulin isotype in human antibody-dependent, cell-mediated cytotoxicity directed by murine monoclonal antibodies. *J Exp Med* **161**, 1-17 (1985).

119. Anasetti, C. et al. Human large granular lymphocytes express high affinity receptors for murine monoclonal antibodies of the IgG3 subclass. *J Immunol* **138**, 2979-81 (1987).

120. Golay, J. et al. CD20 levels determine the in vitro susceptibility to rituximab and complement of B-cell chronic lymphocytic leukemia: further regulation by CD55 and CD59. *Blood* **98**, 3383-9 (2001).

121. Denton, C.P. Leucine Incorporation and Thymidine Incorporation *in Methods in Molecular Biology* (Springer Protocols, Secaucus, NJ, 1997) pg 169-178

122. Barile, F.A., Dierickx, P.J. & Kristen, U. In vitro cytotoxicity testing for prediction of acute human toxicity. *Cell Biol Toxicol* **10**, 155-62 (1994).

123. Ober, R.J., Radu, C.G., Ghetie, V. & Ward, E.S. Differences in promiscuity for antibody-FcRn interactions across species: implications for therapeutic antibodies. *Int Immunol* **13**, 1551-9 (2001).

124. Ghetie, V., Ward, E.S. & Vitetta, E.S. Pharmacokinetics of Antibodies and Immunotoxins in Mice and Humans *in Handbook of Anticancer Pharmacokinetics and Pharmacodynamics* (ed. Figg WD McLeod HL) pg 475-498 (Humana Press Inc, Totowa, NJ, 2004).

125. Waldmann, T.A. Immunotherapy: past, present and future. *Nat Med* **9**, 269-77 (2003).

126. Tedder, T.F., Zhou, L.J. & Engel, P. The CD19/CD21 signal transduction complex of B lymphocytes. *Immunol Today* **15**, 437-42 (1994).

127. Khazaeli, M.B., Conry, R.M. & LoBuglio, A.F. Human immune response to monoclonal antibodies. *J Immunother Emphasis Tumor Immunol* **15**, 42-52 (1994).

128. Zhang, M. et al. Effective therapy for a murine model of human anaplastic large-cell lymphoma with the anti-CD30 monoclonal antibody, HeFi-1, does not require activating Fc receptors. *Blood* **108**, 705-10 (2006).

129. Page, D.M. & DeFranco, A.L. Role of phosphoinositide-derived second messengers in mediating anti-IgM-induced growth arrest of WEHI-231 B lymphoma cells. *J Immunol* **140**, 3717-26 (1988).

130. Nissim, A. & Chernajovsky, Y. Historical development of monoclonal antibody therapeutics. *Handb Exp Pharmacol*, 3-18 (2008).

131. Murphy, M., Jason-Moller, L. & Bruno, J. Using Biacore to measure the binding kinetics of an antibody-antigen interaction. *Curr Protoc Protein Sci* **Chapter 19**, Unit 19 14 (2006).

132. Uchida, J. et al. The innate mononuclear phagocyte network depletes B lymphocytes through Fc receptor-dependent mechanisms during anti-CD20 antibody immunotherapy. *J Exp Med* **199**, 1659-69 (2004).

133. Scheinberg, D.A. & Chapman, P.B. Therapeutic applications of monoclonal antibodies for human diseases *in Monoclonal*

*Antibodies: Principles and Applications* (ed. J.R. Birch and E.S. Lennox) pg 45 (Wiley-Liss, Inc., New York, 1995).

134. Gorter, A. & Meri, S. Immune evasion of tumor cells using membrane-bound complement regulatory proteins. *Immunol Today* **20**, 576-82 (1999).

135. Unkeless, J.C., Scigliano, E. & Freedman, V.H. Structure and function of human and murine receptors for IgG. *Annu Rev Immunol* **6**, 251-81 (1988).

136. van de Winkel, J.G. & Anderson, C.L. Biology of human immunoglobulin G Fc receptors. *J Leukoc Biol* **49**, 511-24 (1991).

137. Reff, M.E. et al. Depletion of B cells in vivo by a chimeric mouse human monoclonal antibody to CD20. *Blood* **83**, 435-45 (1994).

138. McEarchern, J.A. et al. Engineered anti-CD70 antibody with multiple effector functions exhibits in vitro and in vivo antitumor activities. *Blood* **109**, 1185-92 (2007).

139. Scallon, B.J., Moore, M.A., Trinh, H., Knight, D.M. & Ghrayeb, J. Chimeric anti-TNF-alpha monoclonal antibody cA2 binds recombinant transmembrane TNF-alpha and activates immune effector functions. *Cytokine* **7**, 251-9 (1995).

140. Di Gaetano, N. et al. Complement activation determines the therapeutic activity of rituximab in vivo. *J Immunol* **171**, 1581-7 (2003).

141. Seino, J. et al. Activation of human complement by mouse and mouse/human chimeric monoclonal antibodies. *Clin Exp Immunol* **94**, 291-6 (1993).

142. Golay, J. et al. Biologic response of B lymphoma cells to anti-CD20 monoclonal antibody rituximab in vitro: CD55 and CD59 regulate complement-mediated cell lysis. *Blood* **95**, 3900-8 (2000).

143. Ghetie, V. et al. Abnormally short serum half-lives of IgG in beta 2-microglobulin-deficient mice. *Eur J Immunol* **26**, 690-6 (1996).

144. Junghans, R.P. & Anderson, C.L. The protection receptor for IgG catabolism is the beta2-microglobulin-containing neonatal intestinal transport receptor. *Proc Natl Acad Sci U S A* **93**, 5512-6 (1996).

145. Israel, E.J., Wilsker, D.F., Hayes, K.C., Schoenfeld, D. & Simister, N.E. Increased clearance of IgG in mice that lack beta 2-microglobulin: possible protective role of FcRn. *Immunology* **89**, 573-8 (1996).

146. Gokbuget, N. & Hoelzer, D. Treatment of adult acute lymphoblastic leukemia. *Semin Hematol* **46**, 64-75 (2009).

147. Byrd, J.C. et al. Phase 1 study of lumiliximab with detailed pharmacokinetic and pharmacodynamic measurements in patients with relapsed or refractory chronic lymphocytic leukemia. *Clin Cancer Res* **13**, 4448-55 (2007).

148. Leonard, J.P. & Goldenberg, D.M. Preclinical and clinical evaluation of epratuzumab (anti-CD22 IgG) in B-cell malignancies. *Oncogene* **26**, 3704-13 (2007).

149. Ghetie, M.A. et al. Disseminated or localized growth of a human B-cell tumor (Daudi) in SCID mice. *Int J Cancer* **45**, 481-5 (1990).

150. Long, J.M. Treatment approaches and nursing applications for non-Hodgkin lymphoma. *Clin J Oncol Nurs* **11**, 13-21 (2007).

151. Emmanouilides, C. Radioimmunotherapy for non-hodgkin lymphoma : historical perspective and current status. *J Clin Exp Hematop* **47**, 43-60 (2007).

152. Stavenhagen, J.B. et al. Fc optimization of therapeutic antibodies enhances their ability to kill tumor cells in vitro and controls tumor expansion in vivo via low-affinity activating Fcgamma receptors. *Cancer Res* **67**, 8882-90 (2007).

153. Heijnen, I.A. et al. Antigen targeting to myeloid-specific human Fc gamma RI/CD64 triggers enhanced antibody responses in transgenic mice. *J Clin Invest* **97**, 331-8 (1996).

154. Park, S.Y. et al. Resistance of Fc receptor- deficient mice to fatal glomerulonephritis. *J Clin Invest* **102**, 1229-38 (1998).

155. Loisel, S. et al. Relevance, advantages and limitations of animal models used in the development of monoclonal antibodies for cancer treatment. *Crit Rev Oncol Hematol* **62**, 34-42 (2007).

156. Beyersdorf, N. et al. Selective targeting of regulatory T cells with CD28 superagonists allows effective therapy of experimental autoimmune encephalomyelitis. *J Exp Med* **202**, 445-55 (2005).

157. Suntharalingam, G. et al. Cytokine storm in a phase 1 trial of the anti-CD28 monoclonal antibody TGN1412. *N Engl J Med* **355**, 1018-28 (2006).

158. Pegram, M.D., Konecny, G. & Slamon, D.J. The molecular and cellular biology of HER2/neu gene amplification/overexpression and the clinical development of herceptin (trastuzumab) therapy for breast cancer. *Cancer Treat Res* **103**, 57-75 (2000).

159. Carter, P. et al. Humanization of an anti-p185HER2 antibody for human cancer therapy. *Proc Natl Acad Sci U S A* **89**, 4285-9 (1992).

160. Pegram, M. & Ngo, D. Application and potential limitations of animal models utilized in the development of trastuzumab (Herceptin): a case study. *Adv Drug Deliv Rev* **58**, 723-34 (2006).

161. Byrd, J.C. et al. The mechanism of tumor cell clearance by rituximab in vivo in patients with B-cell chronic lymphocytic leukemia: evidence of caspase activation and apoptosis induction. *Blood* **99**, 1038-43 (2002).

162. Petkova, S.B. et al. Enhanced half-life of genetically engineered human IgG1 antibodies in a humanized FcRn mouse model: potential application in humorally mediated autoimmune disease. *Int Immunol* **18**, 1759-69 (2006).

163. Bosma, G.C., Custer, R.P. & Bosma, M.J. A severe combined immunodeficiency mutation in the mouse. *Nature* **301**, 527-30 (1983).

164. Dorshkind, K., Pollack, S.B., Bosma, M.J. & Phillips, R.A. Natural killer (NK) cells are present in mice with severe combined immunodeficiency (scid). *J Immunol* **134**, 3798-801 (1985).